Table 2
Norepinephrine and Na–K-ATPase pump

	Control	Beta	NKA
Norepinephrine			
Plasma (pg/ml)	576±68	654±86	667±74
Left ventricle (ng/g tissue)	2092±193	2208±185	2147±215
Na–K-ATPase activity (μM Pi/h/mg protein)			
Each myocardium	143±20	133±25	94±16*
Foreign myocardium+purified IgG	145±12	138±15	98±12*

* $p<0.03$ vs. control, beta.

or M2-muscarinic receptors could induce cardiac hypertrophy [5,6]. Present study is the first report that repeated immunization using sarcolemmal Na–K-ATPase is able to induce cardiac hypertrophy mimicking DCM in rabbits. However, mechanisms underlying the development of cardiac hypertrophy have not been fully addressed. Inflammatory cell infiltration was observed at the early stage during immunization in previous studies. Our preliminary study also indicated that inflammatory cellular infiltration was observed in ventricular myocardium from rabbits immunized by Na–K-ATPase as well as those immunized by beta-adrenergic receptors 3 months after first immunization [5]. Whereas cellular infiltration in both groups subsided at 6 months, Abs against such antigens were persistently elevated. Our present study indicated antigen-specific production of Abs after myocarditis and that biochemical properties of hypertrophic myocardium were different by immunized antigens.

4.2. Alterations in Na–K-ATPase associated with cardiac hypertrophy

Sarcolemmal Na–K-ATPase activities declined in hypertrophic heart. Not alpha2- but alpha1- and alpha3-subunit of this pump decreased in human failing heart [7]. Protein level of the alpha3-subunit also decreased in high-frequency pacing model and in continuous norepinephrine infusion model [8]. Our present study showed that alpha1-subunit of Na–K-ATPase showed decrease tendency in beta and NKA group compared to the control group. The knockout mouse study indicated that less alpha1-subunit of Na–K-ATPase induced less contractility [9]. Short immunization period was thought as one of the reasons for no significant difference of this isoform in present study. In contrast, alpha3 protein level significantly decreased in NKA group than in other groups. Previous finding has shown that myocardial interstitial norepinephrine content was correlated with alpha3 protein levels [8]. However, myocardial as well as plasma norepinephrine levels were similar in the three groups in present study. As other humoral factor that could influence sarcolemmal Na–K-ATPase activity, there also exists ouabain that was reported to decrease alpha3-subunit mRNA level in vitro but to have no influence against alpha1-isoform [10]. Our preliminary study indicated that there were no differences of peripheral ouabain concentration among three groups.

4.3. Antigen-specific difference of hypertrophic myocardium

We have shown that Abs against Na–K-ATPase antibodies exhibits ouabain-like effects in vitro, inhibiting Na–K-ATPase catalytic activities [11]. And Abs against beta1-adrenergic receptors exhibit sustained sympathomimetic actions [5]. Complement activation is one of common mechanisms of cardiac hypertrophy induced by both Abs, but is not able to explain the difference of myocardial Na–K-ATPase activities in our present study. Our preliminary study using DCM patients' serum suggested that the epitope of anti Na–K-ATPase antibodies was a particular sequence with the alpha3-subunit of this pump. Therefore, we speculated that

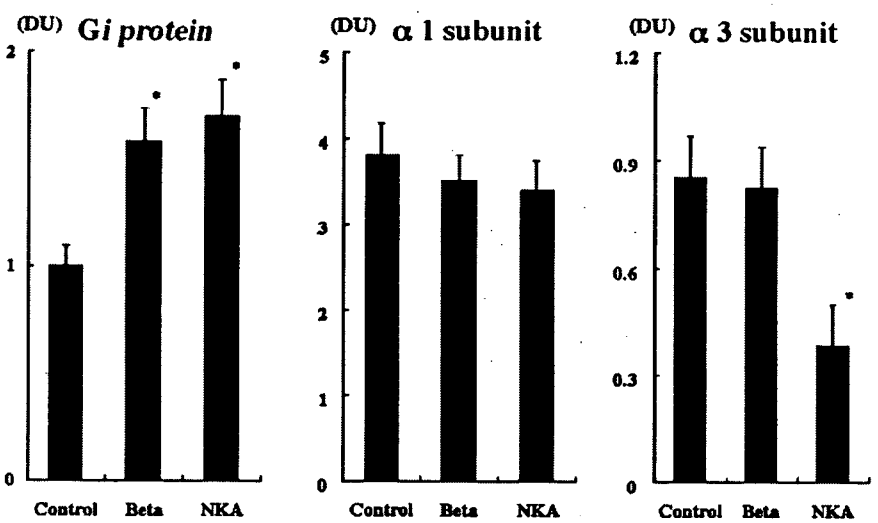

Fig. 4. Densitometric data of Gi protein, alpha1- and alpha3-subunit of Na–K-ATPase on immunoblotting. Beta, NKA and control; same as Fig. 1. DU: densitometric unit. Data are expressed mean±S.D. *$p<0.01$ vs. control.

this bioactive autoantibody would be one of the reasons for downregulation of alpha3-subunit of Na–K-ATPase.

References

[1] Staudt A, Bohm M, Knebel F, et al. Potential role of autoantibodies belonging to the immunoglobulin G-3 subclass in cardiac dysfunction among patients with dilated cardiomyopathy. Circulation 2002; 106:2448–53.

[2] Zwaka TP, Manolov D, Ozdemir C, et al. Complement and dilated cardiomyopathy: a role of sublytic terminal complement complex-induced tumor necrosis factor-alpha synthesis in cardiac myocytes. Am J Pathol 2002;161:449–57.

[3] Baba A, Yoshikawa T, Fukuda Y, et al. Autoantibodies against M2-muscarinic acetylcholine receptors: new upstream targets in atrial fibrillation in patients with dilated cardiomyopathy. Eur Heart J 2004;25:1108–15.

[4] Baba A, Yoshikawa T, Nakamura I, Iwata M, Wainai Y, Ogawa S. Isoform-specific alterations in cardiac and erythrocyte Na^+,K^+-ATPase activity induced by norepinephrine. J Card Fail 1998;4:333–41.

[5] Iwata M, Yoshikawa T, Baba A, et al. Autoimmunity against the second extracellular loop of beta(1)-adrenergic receptors induces beta-adrenergic receptor desensitization and myocardial hypertrophy in vivo. Circ Res 2001;88:578–86.

[6] Matsui S, Fu ML, Katsuda S, et al. Peptides derived from cardiovascular G-protein-coupled receptors induce morphological cardiomyopathic changes in immunized rabbits. J Mol Cell Cardiol 1997;29:641–55.

[7] Schwinger RH, Wang J, Frank K, et al. Reduced sodium pump alpha1, alpha3, and beta1-isoform protein levels and Na+,K+-ATPase activity but unchanged Na+–Ca2+ exchanger protein levels in human heart failure. Circulation 1999;99:2105–12.

[8] Kim CH, Fan TH, Kelly PF, et al. Isoform-specific regulation of myocardial Na,K-ATPase alpha-subunit in congestive heart failure. Role of norepinephrine. Circulation 1994;89:313–20.

[9] Lingrel J, Moseley A, Dostanic I, et al. Functional roles of the alpha isoforms of the Na,K-ATPase. Ann NY Acad Sci 2003;986:354–9.

[10] Huang L, Kometiani P, Xie Z. Differential regulation of Na/K-ATPase alpha-subunit isoform gene expressions in cardiac myocytes by ouabain and other hypertrophic stimuli. J Mol Cell Cardiol 1997;29:3157–67.

[11] Baba A, Yoshikawa T, Ogawa S. Autoantibodies produced against sarcolemmal Na–K-ATPase: possible upstream targets of arrhythmias and sudden death in patients with dilated cardiomyopathy. J Am Coll Cardiol 2002;40:1153–9.

A synthetic small molecule, ONO-1301, enhances endogenous growth factor expression and augments angiogenesis in the ischaemic heart

Kazuto NAKAMURA*†, Masataka SATA*‡, Hiroshi IWATA*, Yoshiki SAKAI§, Yasunobu HIRATA*, Kiyotaka KUGIYAMA† and Ryozo NAGAI*

*Department of Cardiovascular Medicine, University of Tokyo Graduate School of Medicine, 7-3-1 Hongo, Bunkyo-ku, Tokyo 113-8655, Japan, †Second Department of Internal Medicine, Interdisciplinary Graduate School of Medicine and Engineering, University of Yamanashi, 1110 Shimokato, Nakakoma-gun, Yamanashi, 409-3898, Japan, ‡Department of Advanced Clinical Science and Therapeutics, University of Tokyo Graduate School of Medicine, 7-3-1 Hongo, Bunkyo-ku, Tokyo 113-8655, Japan, and §Ono Pharmaceutical Company Ltd, 2-1-5 Doshomachi, Chuo-ku, Osaka 541-8526, Japan

ABSTRACT

It has been shown previously that administration of angiogenic growth factors as genes or proteins can augment collateral growth in ischaemic tissues. In the present study, we have investigated the effect of ONO-1301, a synthetic prostacyclin agonist with thromboxane-synthase-inhibitory activity, on expression of endogenous growth factors and angiogenesis. ONO-1301 induced secretion of HGF (hepatocyte growth factor) and VEGF (vascular endothelial growth factor) from cultured normal human dermal fibroblasts in a dose-dependent manner. Dibutyryl cAMP, an analogue of cAMP, and forskolin, an adenylate cyclase activator, mimicked the effect of ONO-1301. Conversely, Rp-cAMP (adenosine 3′,5′-cyclic monophosphorothioate), an inhibitor of cAMP, partially inhibited the effect of ONO-1301, suggesting that cAMP mediated the effect of ONO-1301 in up-regulating the expression of HGF and VEGF, at least in part. ONO-1301 promoted tube-like formation by HUVECs (human umbilical vein endothelial cells) when co-cultured with fibroblasts, and the angiogenic effect of ONO-1301 was abrogated by administration of a neutralizing antibody against HGF or VEGF. To generate a slow-releasing form of ONO-1301, ONO-1301 was mixed with poly(DL-lactic-co-glycolic acid). The slow-releasing form of ONO-1301 was injected directly into the ischaemic myocardium of mice immediately after ligation of the left anterior descending artery. The slow-releasing form of ONO-1301 up-regulated HGF and VEGF expression and increased capillary density in the border zone (342.7 ± 29.7 capillaries/mm^2 in controls compared with 557.2 ± 26.7 capillaries/mm^2 in treated animals; $P < 0.01$) at 7 days. The slow-releasing form of ONO-1301 ameliorated left ventricular enlargement after 28 days and improved survival rate. In conclusion, our results indicate that ONO-1301 up-regulated endogenous growth factors and promoted angiogenesis in response to acute ischaemia. Therefore ONO-1301 might have a therapeutic potential in treating ischaemic diseases.

Key words: angiogenesis, cardiovascular system, hepatocyte growth factor (HGF), ischaemia, prostacyclin, regenerative medicine, vascular endothelial growth factor (VEGF).

Abbreviations: EBM, endothelial growth medium; FBS, fetal bovine serum; FS, fractional shortening; HASMC, human aortic smooth muscle cell; HGF, hepatocyte growth factor; HUVEC, human umbilical vein endothelial cell; LV, left ventricular; LVEDD, LV end-diastolic diameter; LVESD, LV end-systolic diameter; MI, myocardial infarction; NHDF, normal human dermal fibroblast; PG, prostaglandin; PLGA, poly(DL-lactic-co-glycolic acid); Rp-cAMP, adenosine 3′,5′-cyclic monophosphorothioate; RT-PCR, reverse transcriptase-PCR; SR-ONO, slow-releasing form of ONO-1301; VEGF, vascular endothelial growth factor.

Correspondence: Dr Masataka Sata, at the Department of Cardiovascular Medicine, University of Tokyo Graduate School of Medicine, 7-3-1 Hongo, Bunkyo-ku, Tokyo 113-8655, Japan (email msata-circ@umin.net).

INTRODUCTION

Therapeutic angiogenesis has emerged as a promising therapy to treat ischaemic cardiovascular diseases [1]. Administration of growth factors as genes or recombinant proteins has been shown to significantly augment collateral growth in ischaemic tissues [2]. Recent evidence suggests that transplantation of endothelial progenitor cells or total bone marrow cells augments collateral development of ischaemic tissues [3]. As the number of incorporated cells with an endothelial phenotype in ischaemic tissues is generally quite low [4], it was hypothesized that the release of pro-angiogenic factors may mediate the efficacy of autologous cell transplantation [5]. Thus supplementation of angiogenic cytokines may represent a standard strategy in therapeutic angiogenesis. Although it remains to be determined which factor(s) would be the most efficient for clinical use [6], it has been suggested that a combination of several cytokines might be more effective [7].

PGs (prostaglandins) consist of a variety of bioactive substances that play an important role in maintaining local tissue homoeostasis and evoking inflammatory responses. Interestingly, some PGs and their analogues have been shown to stimulate expression of growth factors or cytokines *in vitro* and *in vivo* [8–12]. Matsumoto et al. [8] reported that HGF (hepatocyte growth factor) production by fibroblasts was strongly induced by PGE_1 and prostacyclin, but only slightly by PGE_2 and PGD_2, through transcriptional activation of the HGF gene. It was hypothesized that PGE_1 and prostacyclin, rapidly synthesized after tissue injury, may have a role in tissue repair by inducing HGF expression [8]. In fact, exogenous administration of prostacyclin or its analogues has been shown to protect ischaemic myocardium *in vivo* [13,14]. Indeed, prostacyclin is the major PG released from the ischaemic heart [15]. Prostacyclin analogues have been reported to induce VEGF (vascular endothelial growth factor) expression and enhance angiogenesis *in vivo* in a mouse cornea model [16].

ONO-1301 is a synthetic prostacyclin agonist lacking the typical prostanoid structures, including a five-membered ring and allylic alcohol [17–20]. Prostacyclin and its analogues are not stable *in vivo*, because 15-hydroxyPG dehydrogenase metabolizes their prostanoid structures. In contrast, ONO-1301 is chemically and biologically stable because of the absence of prostanoid structures. Notably, ONO-1301 has thromboxane-synthase-inhibitory activity, because of the presence of a 3-pyridine radical. ONO-1301 exerts long-lasting prostacyclin activity when administered *in vivo* [17–20].

In the present study, we have investigated the effect of ONO-1301 on expression of endogenous growth factors and angiogenesis. ONO-1301 successfully up-regulated the expression of endogenous VEGF and HGF *in vitro* and *in vivo*. Local administration of a slow-releasing form of ONO-1301 augmented angiogenesis and ameliorated LV (left ventricular) enlargement after acute MI (myocardial infarction). Our findings suggest that up-regulation of endogenous growth factors with a small molecule might be useful in therapeutic angiogenesis.

MATERIALS AND METHODS

Animals

Adult male CD1 inbred mice were purchased from SLC Japan [21]. Blood pressure and pulse rate of each mouse were measured with a tail-cuff system (BP-98A; Softron) in conscious animals. In each animal, the mean value of three measurements was used for comparison. All experimental procedures and protocols were approved by the Animal Care and Use Committee of the University of Tokyo and complied with the Guide for the Care and Use of Laboratory Animals (NIH publication No. 86-23, revised 1985).

ONO-1301 and generation of its slow-releasing form

ONO-1301 was synthesized by ONO Pharmaceutical Co. Ltd as described previously [17–20]. A slow-releasing form of ONO-1301 (SR-ONO) was generated by polymerizing ONO-1301 with PLGA [poly(DL-lactic-co-glycolic acid)]. Briefly, ONO-1301 (5 mg) was mixed with 100 mg of PLGA (M_r, 20000; Wako) in 0.1 % polyvinyl alcohol (1:1 molar ratio of PLGA/glycolic acid). Pellets were washed in distilled water several times and freeze-dried. Particle size of SR-ONO was approx. 25–30 μm in diameter, as determined by a Coulter counter. The releasing rate of ONO-1301 PLGA in 0.2 % Tween 80/sodium phosphate buffer was determined by measuring residual ONO-1301 in the pellets.

Measurement of growth factors produced from cultured human fibroblasts

NHDFs (normal human dermal fibroblasts), purchased from Kurabo, were cultured on 48-well plates in DMEM (Dulbecco's modified Eagle's medium; Sigma) containing 10 % (v/v) FBS (fetal bovine serum). Cells were serum-starved for 24 h and were cultured in the absence or presence of ONO-1301 (0.01–1 μmol/l) for 72 h. Dibutyryl cAMP (Sigma), forskolin (Sigma) or Rp-cAMP (adenosine 3′,5′-cyclic monophosphorothioate; Calbiochem) was added to the medium at the concentrations indicated ($n = 3$ for each group). HUVECs (human umbilical vein endothelial cells), purchased from Cambrex, were cultured on 48-well plates in EBM (endothelial growth medium; Cambrex) containing 2 % (v/v) FBS and endothelial cell growth supplements. HUVECs were serum-starved for 24 h and were cultured in EBM with 0.2 % (v/v) FBS in the absence or presence of ONO-1301 (1 μmol/l) for 72 h ($n = 3$ for each group). HASMCs (human aortic smooth muscle cells), purchased

from Kurabo, were cultured on 48-well plates in human smooth muscle cell growth medium (HuMedia-SG2; Kurabo) containing 5% (v/v) FBS and smooth muscle cell growth supplements. HASMCs were serum-starved for 24 h and were cultured in HuMedia-SG2 with 0.5% (v/v) FBS in the absence or presence of ONO-1301 (1 μmol/l) for 72 h ($n = 3$ for each group). Supernatants were harvested to measure concentrations of VEGF and HGF by ELISA (Quantikine; R&D Systems). Total RNA was extracted at 6 h after stimulation. Cells from passages 4–7 were used throughout the study.

Measurement of angiogenic activity *in vitro*

An *in vitro* angiogenesis kit (KZ-1000; Kurabo), consisting of a two-dimensional co-culture system of HUVECs/NHDFs on a 24-well plate, was used according to the manufacturer's instructions [22]. Cells were cultured in the absence or presence of ONO-1301 (0.1 μmol/l), a neutralizing anti-(human HGF) antibody (10 μg/ml; generously given by Dr George F. Vande Woude, Laboratory of Molecular Oncology, Van Andel Institute, Grand Rapids, MI, U.S.A.) [23] and a neutralizing monoclonal anti-(human VEGF) antibody (5 μg/ml; mouse IgG2B, clone 26503; R&D Systems), which recognizes human $VEGF_{165}$ and $VEGF_{121}$. Human recombinant $VEGF_{165}$ (KZ-1300; Kurabo) and human recombinant HGF (294-HG; Kurabo) were used as positive controls in the tube-formation assays. Suramin (Kurabo), an antitrypanosomal agent, was used as an inhibitor of angiogenesis [24]. At 11 days, cells were fixed with 10% formalin and stained using an anti-CD31 antibody. The length of CD31-positive endothelial cells of tube-like structures was quantified in five random high-power fields (×40 magnification) in a blinded fashion using an image analysing system (Kurabo). All assays were performed in triplicate.

Injection of SR-ONO into ischaemic myocardium

MI was induced in 8–10-week-old male CD-1 mice, weighing 35–40 g, by ligating the left anterior descending coronary artery, as described previously [25]. Briefly, mice were anaesthetized by intraperitoneal injection of pentobarbital (50 mg/kg of body weight). A 24-gauge polyethylene tube was inserted into the trachea and mechanical ventilation was provided by a rodent ventilator (SAR-830; CWE). The chest was opened and the heart was exposed. The left descending coronary artery was ligated by 7-0 nylon suture. Immediately after ligation, 2 mg of SR-ONO ($n = 31$), suspended in 50 μl of normal saline with 0.2% Tween 80, was injected directly into the anterior and lateral myocardium around the ischaemic border zone. A total of 2 mg of PLGA microspheres containing no ONO-1301 ($n = 29$) was injected as a control. During the study period of 4 weeks, cages were inspected daily for survival analysis after MI. A neutralizing polyclonal goat anti-(mouse VEGF) antibody (0.0025 μg/kg of body weight; R&D system), which recognizes mouse $VEGF_{164}$ and $VEGF_{120}$, or normal goat IgG (0.025 μg/kg of body weight) was administered intraperitoneally at 0, 3, 5 and 7 days.

Echocardiography

Echocardiographic studies were performed under anaesthesia with pentobarbital (50 mg/kg of body weight) before surgery and at 1 and 28 days after MI [26]. An echocardiography system (EnVisor M2540A; Philips Medical System) was used with a dynamically focused 15 MHz linear-array transducer with a depth setting of 1.5 cm. The resolution provided by 15 MHz linear-array transducers has been reported to be high enough to measure LV diameter in a mouse heart beating at a high rate [27]. Two-dimensional images and M-mode tracings were recorded from the short-axis view at the high papillary muscle level. Care was taken not to apply too much pressure to the chest wall. Measurements were done for at least ten beats in a blinded fashion and repeated twice. LVEDD (LV end-diastolic diameter) and LVESD (LV end-systolic diameter) were measured. FS (fractional shortening) was calculated using the following equation: $FS\ (\%) = (LVEDD - LVESD)/LVEDD \times 100$.

Histological analysis

For histological analysis, mice were killed by intraperitoneal injection of an overdose of sodium pentobarbital at 7 or 28 days. The hearts were carefully removed and fixed with 10% neutral formalin by perfusion fixation. Fixed hearts were cut into three transverse sections from the ligated site of left coronary artery to the apex and embedded in paraffin. Sections (5 μm) were deparaffinized and stained with H&E (haematoxylin and eosin). Immunohistochemistry was performed as described previously [28]. The hearts were fixed overnight in methanol and embedded in paraffin. Sections (5 μm) were deparaffinized and incubated with a rat monoclonal antibody against murine CD31 (clone MEC13.3; BD PharMingen). Antibody binding was visualized using avidin–biotin and the Vector Red chromogenic substrate (Vector Laboratories), followed by counterstaining with haematoxylin. Capillaries were identified by positive staining for anti-CD31 antibody and morphology. The number of capillaries/mm^2 was counted in regions with transversely sectioned myocytes in the border (peri-infarct) zone. Three or four fields in the border zone per section were analysed for each mouse (a total of 10–12 fields/heart) at × 200 magnification [29,30]. Additional sections were counterstained with haematoxylin.

RT-PCR (reverse transcriptase-PCR)

Total RNA was prepared from both ischaemic and non-ischaemic myocardium using RNA Bee (Tel-Test) [31]. RT-PCR was performed as described previously [31]. First-strand cDNA was synthesized from 1 μg of total RNA, using oligo-$(dT)_{20}$ primer and MMLV (Moloney-murine-leukaemia virus)-derived reverse transcriptase (ReverTra Ace-α; Toyobo). A portion (1/20) of the reaction mixture was used as a template for PCR amplification. The mouse VEGF primers, 5′-GCGGGCTGCCTCGCAGTC-3′ (sense) and 5′-TCACCGCCTTGGCTTGTCAC-3′ (antisense), yielded products of 716 bp ($VEGF_{188}$), 644 bp ($VEGF_{164}$) and 512 bp ($VEGF_{120}$). PCR reactions were carried out for 30 cycles with 1 min of denaturation at 94 °C, 1 min of annealing at 65 °C and 1.5 min of extension at 72 °C, followed by 10 min of final extension. The mouse HGF primers, 5′-GCGGGCTGCCTCGCAGTC-3′ (sense) and 5′-TCACCGCCTTGGCTTGTCAC-3′ (antisense), yielded a product of 423 bp (HGF). PCR reactions were carried out for 30 cycles with 1 min of denaturation at 94 °C, 1 min of annealing at 55 °C and 1.5 min of extension at 72 °C, followed by 10 min of final extension [32]. The human VEGF primers, 5′-GGACATCTTCCAGGAGTA-3′ (sense) and 5′-TGCAACGAGAGTCTGTGT-3′ (antisense), yielded products of 413 bp and 341 bp. PCR reactions were carried out for 30–35 cycles with 30 s of denaturation at 94 °C, 30 s of annealing at 60 °C and 30 s of extension at 72 °C, followed by 10 min of final extension. The human HGF primers, 5′-ATGCTCATGGACCCTGGT-3′ (sense) and 5′-GCCTGGCAAGCTTCATTA-3′ (antisense), yielded a product of 423 bp (HGF). PCR reactions were carried out for 30 cycles with 30 s of denaturation at 94 °C, 30 s of annealing at 60 °C and 1 min of extension at 72 °C, followed by 10 min of final extension.

Statistics

All values are means ± S.E.M. Multiple comparisons were performed by one-way ANOVA with Fisher's post-hoc comparison. Survival analysis was performed by Kaplan–Meier analysis and evaluated by log-rank test. A value of $P < 0.05$ was considered to be statistically significant.

RESULTS

Effect of ONO-1301 on HGF and VEGF secretion

NHDFs were cultured on 48-well plates in the absence or presence of ONO-1301. ONO-1301 (1 μmol/l) increased the concentration of HGF and VEGF in the medium in a time-dependent manner, with a maximum response being obtained after 72 h (results not shown). Treatment with ONO-1301 (0.01–1 μmol/l) for 72 h increased HGF and VEGF concentrations in a dose-dependent manner (Figures 1A and 1B). Dibutyryl cAMP (0.5 mmol/l), an analogue of cAMP, and forskolin (1 μmol/l), an adenylate cyclase activator, mimicked the effect of ONO-1301 (Figures 1C and 1D). Rp-cAMP (0.5 mmol/l), a cAMP inhibitor, partially inhibited the effect of ONO-1301 (Figure 1E). These results suggested that cAMP, at least in part, mediated the effect of ONO-1301 in up-regulating HGF. When a neutralizing anti-HGF antibody was added, ONO-1301 failed to up-regulate VEGF expression in fibroblasts, suggesting that HGF may mediate ONO-1301-induced stimulation of VEGF production (Figure 1F). Furthermore, to investigate the effect of ONO-1301 on growth factor secretion in other cell types, the effect of ONO-1301 on HUVECs and HASMCs was examined. Up-regulation of HGF or VEGF was not be detected in ONO-1301-treated HUVECs as determined by ELISA (Figures 1G and 1H) or RT-PCR (results not shown). On the other hand, HASMCs produced HGF and VEGF abundantly, and ONO-1301 slightly, but significantly, up-regulated HGF secretion (Figure 1G).

Effect of ONO-1301 on *in vitro* angiogenesis

The angiogenic activity of ONO-1301 *in vitro* was evaluated using a two-dimensional co-culture system of HUVECs and NHDFs. ONO-1301 enhanced tube-like formation by HUVECs (Figure 2A). The angiogenic activity of ONO-1301 was comparable with that of VEGF or HGF. The angiogenic effect of ONO-1301 was reduced by administration of neutralizing anti-HGF or anti-VEGF antibodies. These findings suggested that the favourable effect of ONO-1301 on angiogenesis *in vitro* was mediated, at least in part, by up-regulation of HGF and VEGF.

Effect of ONO-1301 on endogenous growth factor expression in ischaemic myocardium

To deliver ONO-1301 locally and chronically, ONO-1301 was polymerized with PLGA to generate SR-ONO. The *in-vitro*-releasing test revealed that ONO-1301 was released continuously from SR-ONO within 12–14 days (Figure 3A). When the effect of PLGA and SR-ONO on growth factor secretion was tested, PLGA had no effect on HGF and VEGF expression (Figure 3B), whereas SR-ONO up-regulated secretion of both growth factors (Figure 3B). The angiogenic effect of ONO-1301 *in vivo* was evaluated by injecting SR-ONO into ischaemic myocardium immediately after ligation of the left anterior descending artery. No systemic effects, including those on blood pressure and heart rate, were observed following the local injection of SR-ONO into the heart. Expression of HGF and VEGF was analysed by RT-PCR in ischaemic and non-ischaemic areas at 7 days

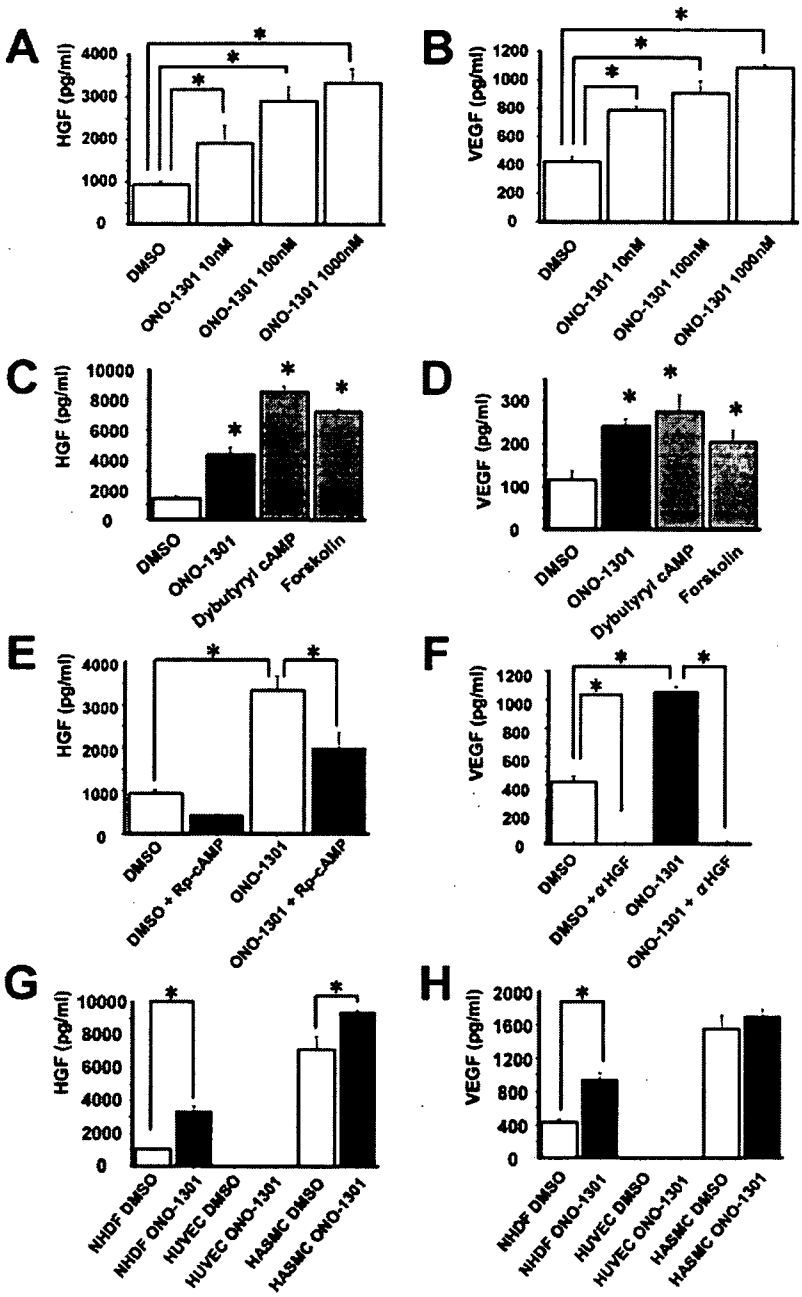

Figure 1 Effect of ONO-1301 on HGF and VEGF production

(A and B) NHDFs were cultured in the absence or presence of ONO-1301 (0.01–1 μmol/l) for 72 h. (C and D) NHDFs were cultured on a 48-well plate in the absence or presence of ONO-1301 (0.1 μmol/l), dibutyryl cAMP (0.5 mmol/l) and forskolin (1 μmol/l) for 72 h. (E) NHDFs were cultured with vehicle and ONO-1301 alone (1 μmol/l) or in combination with Rp-cAMP (0.5 nmol/l) for 72 h. (F) NHDFs were cultured with vehicle and ONO-1301 alone (1 μmol/l) or in combination with a neutralizing anti-HGF antibody (αHGF; 20 μg/ml) for 72 h. (G and H) HUVECs and HASMCs were cultured in the absence or presence of ONO-1301 (1 μmol/l) for 72 h. Following treatment, HGF (A, C, E and G) and VEGF (B, D, F and H) concentrations in the supernatants were determined by ELISA. In each panel, values are means $\pm$ S.E.M. of two or three replicate measurements. $^*P < 0.05$.

after MI (Figure 3C). HGF mRNA was down-regulated in the ischaemic myocardium treated with vehicle, and SR-ONO partially restored the expression. VEGF expression was not detected in the non-ischaemic myocardium, but endogenous VEGF expression was slightly up-regulated in the ischaemic myocardium treated with vehicle. SR-ONO up-regulated VEGF expression further in ischaemic myocardium (Figure 3C).

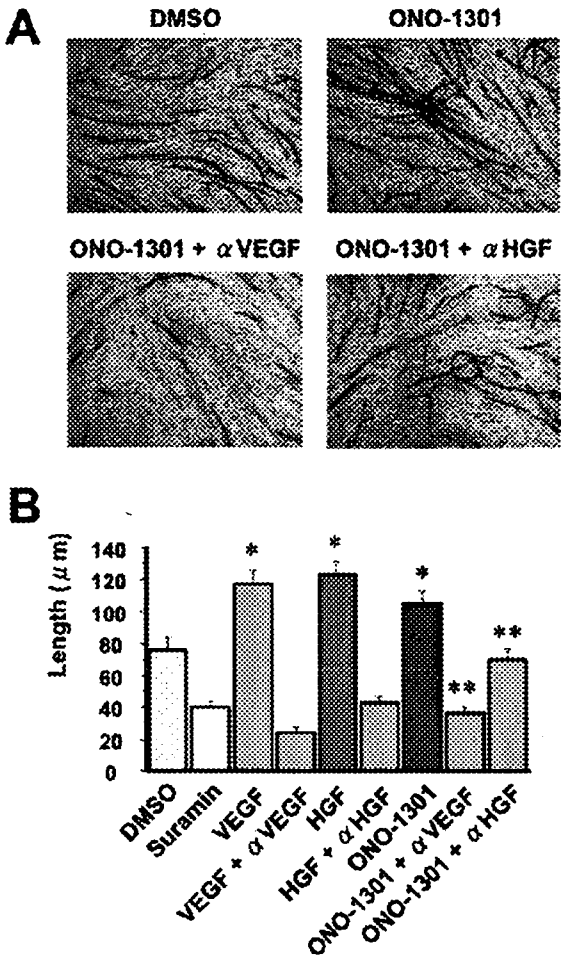

Figure 2 Promotion of *in vitro* tube formation by ONO-1301

(A) *In vitro* angiogenic activity of ONO-1301 was evaluated in the absence or presence of ONO-1301 (0.1 μmol/l), a neutralizing anti-(human HGF) antibody (αHGF; 10 μg/ml) and a neutralizing anti-(human VEGF) antibody (αVEGF; 5 μg/ml). At 11 days, cells were fixed with 10% formalin and stained using an anti-CD31 antibody. (B) Length of CD31-positive endothelial cells with tube-like structures was quantified in five random high-power fields ($\times$ 40 magnification) in a blinded fashion using an image analysing system ($n = 3$ for each group). Values are means $\pm$ S.E.M. $^*P < 0.05$ compared with control (DMSO); $^{**}P < 0.05$ compared with ONO-1301 alone.

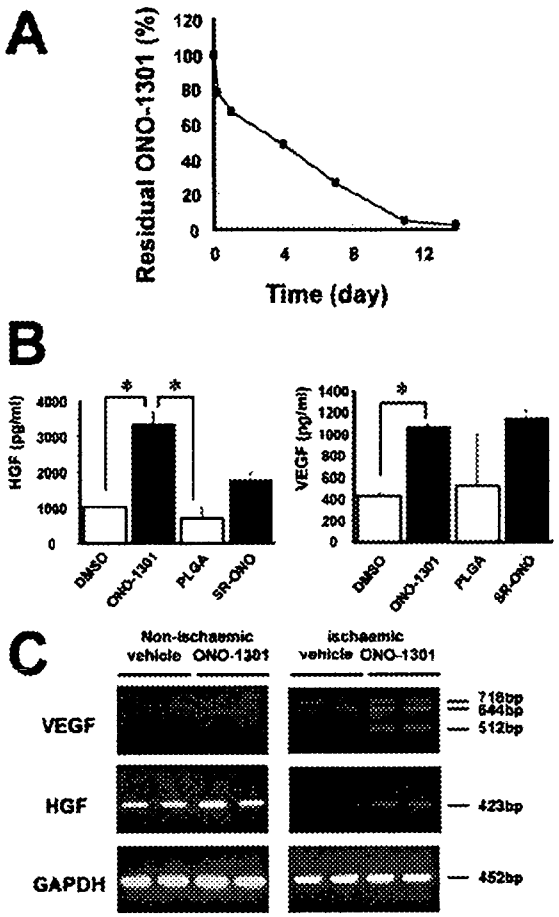

Figure 3 Up-regulation of HGF and VEGF expression by SR-ONO

(A) The releasing rate of the ONO-1301–PLGA complex in 0.2% Tween 80/sodium phosphate buffer was determined by measuring residual ONO-1301 in the pellets. (B) The effect of ONO-1301, PLGA and SR-ONO on growth factor secretion. ONO-1301 (1 μmol/l), PLGA (9 μg/ml) or SR-ONO (equivalent to 1 μmol/ml ONO-1301) were added to NHDFs. Supernatants were harvested after 72 h and HGF and VEGF concentrations were determined. $^*P < 0.05$. (C) Immediately after coronary ligation, 2 mg of SR-ONO was injected directly into the myocardium ($n = 5$). PLGA (2 mg) containing no ONO-1301 was injected as a control ($n = 5$). Total RNA was isolated at 7 days and RT-PCR was performed. GAPDH, glyceraldehyde-3-phosphate dehydrogenase.

Effect of ONO-1301 on angiogenesis in ischaemic myocardium

Anti-CD31 immunostaining revealed that SR-ONO significantly increased capillary density in the ischaemic border zone at 7 days after MI (Figure 4A). The angiogenic effect of SR-ONO was partially abrogated by a neutralizing anti-(mouse VEGF) antibody (Figure 4B), suggesting that ONO-1301 augmented angiogenesis, at least in part, via the up-regulation of VEGF.

Effect of ONO-1301 on LV dilatation and survival after MI

LV function was evaluated by echocardiography at 0, 1 and 28 days after MI (Figure 5A). SR-ONO significantly attenuated LV remodelling at 28 days after MI, as determined by increased LVEDD and LVESD (Figure 5B). The survival rate up to 2 weeks after MI was significantly improved by SR-ONO ($P < 0.05$; Figure 6A). The beneficial effects of ONO-1301 were abrogated by administration of an anti-VEGF antibody (Figure 6B).

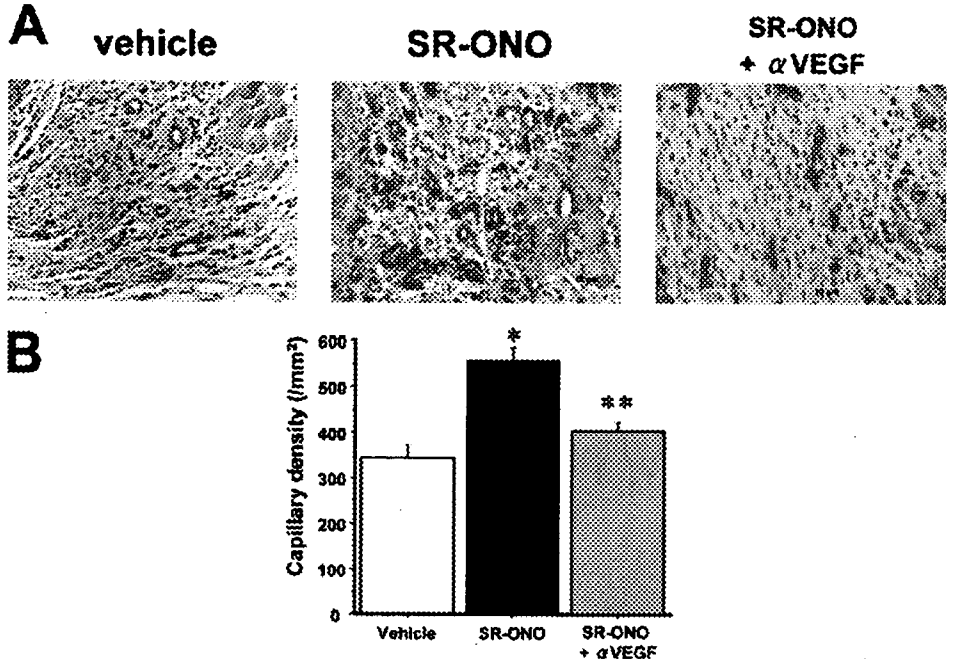

Figure 4 Increased capillary density at the border zone by ONO-1301 at 7 days after MI

(A) Capillary density at border zone at 7 days after treatment with vehicle and SR-ONO alone or in combination with a neutralizing anti-(human VEGF) antibody (SR-ONO + αVEGF). Endothelial cells were visualized using an anti-CD31 antibody and avidin–biotin and Vector Red chromogenic substrate, followed by counterstaining with haematoxylin. Magnification, × 200. (B) Capillaries were identified by positive staining for anti-CD31 antibody and morphology ($n = 5$ for each group). The number of capillaries/mm^2 was counted in regions with transversely sectioned myocytes in the border (peri-infarct) zone. Three or four fields in the border zone per section were analysed in each mouse (a total of approx. 10–12 fields/heart) at × 200 magnification. Values are means ± S.E.M. *$P < 0.01$ compared with vehicle; **$P < 0.05$ compared with SR-ONO.

DISCUSSION

In the present study, we have demonstrated that ONO-1301 induced the production of endogenous HGF and VEGF *in vitro* and *in vivo*. Injection of SR-ONO augmented angiogenesis in ischaemic myocardium and prevented LV enlargement. ONO-1301 also significantly improved survival after MI. The beneficial effects of ONO-1301 were abrogated by administration of a neutralizing antibody against VEGF.

Therapeutic angiogenesis has emerged as a promising strategy to treat ischaemic diseases. Administration of angiogenic growth factors as proteins or genes enhances collateral formation; however, previous studies have suggested that new vessels regenerated by the overexpression of a single growth factor are not fully functional [33,34], suggesting that a combination of several cytokines are required to regenerate physiological collateral arteries [7,35]. It has been reported that transplantation of bone marrow cells or circulating progenitor cells promotes new vessel formation in ischaemic tissues [3,36,37]. Bone-marrow-derived cells accumulate around growing collateral arteries with expression of several growth factors and chemokines [4,38]. It was hypothesized that bone-marrow-derived cells promote vascular growth not only by incorporating into vessel walls, but also by secreting several cytokines [4,5]. It is likely that an increase in the local concentration of growth factors at the site of ischaemia would favour collateral formation. Therefore stimulation of local residual cells to produce growth factors could be an alternative strategy to supply growth factors to the site of new vessel formation. In fact, it has been reported that cell transplantation stimulates ischaemic muscle to secrete angiogenic cytokines [39].

It has been shown that PGs regulate HGF expression from cultured cells [8,40]. HGF production was transcriptionally activated by PGE_1 and PGI_2, but only slightly by PGE_2 and PGD_2, in cultured human skin fibroblasts and smooth muscle cells [8,40]. In addition, administration of PGE_1 increased circulating HGF levels in patients with peripheral arterial disease [11]. It has been suggested that the generation of HGF is induced through a cAMP-mediated pathway [41], and a cAMP-responsive element consensus sequence has been located in the promoter region of the HGF gene [32]. HGF induces VEGF expression in smooth muscle cells [42,43] and keratinocytes [44], and Sakurai et al.

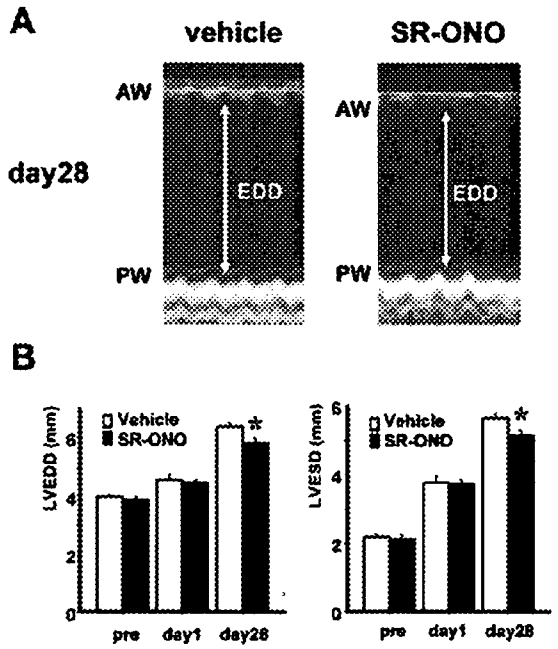

Figure 5 Amelioration of LV dilation by SR-ONO

Echocardiographic studies were performed under anaesthesia before surgery (pre) and at 1 and 28 days after MI ($n = 8$ for each group), and LVEDD and LVESD were measured. (A) Representative M-mode echocardiograms obtained from mice treated with vehicle and SR-ONO at 28 days after MI. AW, LV anterior wall; PW, LV posterior wall. (B) Quantification of LVEDD and LVESD in mice treated with vehicle or SR-ONO for up to 28 days after MI. Values are means ± S.E.M., $n = 8$ for each group. $^*P < 0.05$ compared with vehicle at day 28.

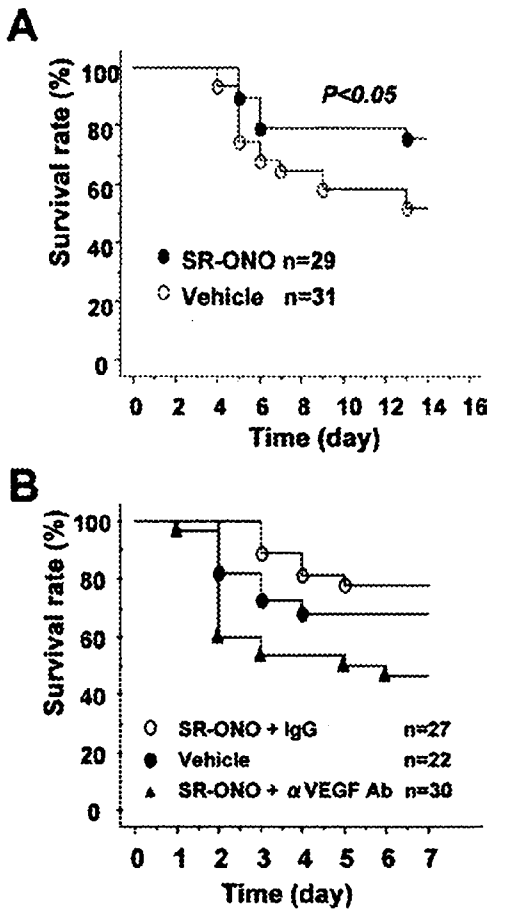

Figure 6 Kaplan–Meier survival analysis after MI in mice treated with vehicle or SR-ONO

MI was induced in 8–10-week-old male CD-1 mice and, immediately after ligation, vehicle (2 mg of PLGA microspheres) or SR-ONO (2 mg) was injected directly into the ischaemic myocardium. In (B), a neutralizing anti-(mouse VEGF) antibody (αVEGF Ab; 0.0025 μg/kg of body weight) or normal goat IgG (0.025 μg/kg of body weight) was administered intraperitoneally at 0, 3, 5 and 7 days. (A) The percentage of surviving mice treated with vehicle ($n = 31$) or SR-ONO ($n = 29$). (B) The percentage of surviving mice treated with vehicle ($n = 22$), SR-ONO + normal Ig ($n = 27$) or SR-ONO + αVEGF ($n = 30$). The difference between the groups was tested by the log-rank test.

[45] have shown that PGs stimulated retinal capillary pericyte proliferation with the induction of c-fos mRNA, phosphorylation of CREB (cAMP-response-element-binding protein) and increased expression of VEGF. Induction of VEGF by PGs was almost completely blocked by SQ22536, an adenylate cyclase inhibitor, suggesting that HGF production via the cAMP pathway is the major signalling pathway for the induction of VEGF mRNA by PGs. Thus local administration of PGs appears to effectively induce the production of HGF by local residual cells. HGF subsequently up-regulates VEGF. In the present study, ONO-1301, a synthetic non-prostanoid prostacyclin agonist, successfully up-regulated the expression of VEGF and HGF *in vitro* and *in vivo*. The effect of ONO-1301 was mimicked by a cAMP analogue or cAMP-elevating reagent and was inhibited by a cAMP inhibitor, suggesting that cAMP mediates the beneficial effect of ONO-1301, at least in part.

The prostanoid structure in prostacyclin and its analogues is subjected to metabolism by 15-hydroxyPG dehydrogenase. A phase I clinical trial investigating the oral administration of ONO-1301 has been stopped due to a high incidence of diarrhoea (Y. Sakai, unpublished work), possibly due to stimulation of gastrointestinal cells. Systemic administration of ONO-1301 also caused hypotension in mice and rats (Y. Sakai, unpublished work). To overcome these potential side effects caused by oral administration of ONO-1301, we generated SR-ONO with PLGA. PLGA can be gradually absorbed without tissue damage. We did not observe vasodilatation or hypotension, which was reported following systemic administration of a high dose of prostacyclin [46], its analogues or ONO-1301 (Y. Sakai, unpublished work).

Thus SR-ONO appears to enable ONO-1301 to be delivered locally and chronically at the site of ischaemia with minimum adverse systemic effects. For therapeutic use, it would be feasible to optimize the size of the microspheres, the time of drug release and the content of ONO-1301.

In ischaemic hearts, a slight up-regulation of VEGF was observed, which was significantly enhanced by SR-ONO. In contrast, HGF was constitutively expressed by non-ischaemic myocardium and was down-regulated in ischaemic myocardium, a finding consistent with previous studies showing that hypoxic treatment resulted in a significant decrease in local HGF production and a increase in VEGF expression in various cell types [47]. SR-ONO attenuated this ischaemic-induced down-regulation of HGF.

Results from the *in vitro* experiments suggested that growth factors were not induced in endothelial cells, although we could not perform immunohistochemistry to identify which cell types secreted growth factors in the ischaemic heart. It is plausible that growth factors secreted by neighbouring fibroblasts and smooth muscle cells stimulated residual endothelial cells in a paracrine manner.

ONO-1301 prevented LV dilatation with no significant effect on ejection fraction. The preventive effect of ONO-1301 on cardiac remodelling was relatively small when observed at 28 days after MI; however, ONO-1301 significantly increased the capillary density in the ischaemic heart. We also observed that ONO-1301 attenuated myocardial hypertrophy and fibrosis in the intact myocardium (results not shown). Further studies are required to evaluate the long-term effect of ONO-1301 on cardiac function in a chronic myocardial ischaemia model.

In summary, we have demonstrated that ONO-1301 stimulated fibroblasts to secrete angiogenic cytokines. SR-ONO up-regulated HGF and VEGF and promoted angiogenesis in ischaemic mouse hearts. Administration of synthetic small molecules is apparently less invasive than isolation and transplantation of endothelial progenitor cells and/or bone marrow cells. Repeated administration would be easy with a small synthetic molecule, in contrast with autologous bone marrow transplantation that requires bone marrow aspiration. Therefore ONO-1301 might have therapeutic potential in treating ischaemic diseases.

ACKNOWLEDGMENTS

This study was supported, in part, by grants from the Ministry of Education, Culture, Sports, Science and Technology, and the Ministry of Health, Labor and Welfare of Japan. Y.S. is an employee of Ono Pharmaceutical Company Ltd.

REFERENCES

1 Freedman, S. and Isner, J. M. (2001) Therapeutic angiogenesis for ischemic cardiovascular disease. J. Mol. Cell. Cardiol. **33**, 379–393
2 Losordo, D. W. and Dimmeler, S. (2004) Therapeutic angiogenesis and vasculogenesis for ischemic disease: part I: angiogenic cytokines. Circulation **109**, 2487–2491
3 Khakoo, A. Y. and Finkel, T. (2005) Endothelial progenitor cells. Annu. Rev. Med. **56**, 79–101
4 Ziegelhoeffer, T., Fernandez, B., Kostin, S. et al. (2004) Bone marrow-derived cells do not incorporate into the adult growing vasculature. Circ. Res. **94**, 230–238
5 O'Neill, IV T. J., Wamhoff, B. R., Owens, G. K. and Skalak, T. C. (2005) Mobilization of bone marrow-derived cells enhances the angiogenic response to hypoxia without transdifferentiation into endothelial cells. Circ. Res. **97**, 1027–1035
6 Hughes, G. C., Biswas, S. S., Yin, B. et al. (2004) Therapeutic angiogenesis in chronically ischemic porcine myocardium: comparative effects of bFGF and VEGF. Ann. Thorac. Surg. **77**, 812–818
7 Yamauchi, A., Ito, Y., Morikawa, M. et al. (2003) Pre-administration of angiopoietin-1 followed by VEGF induces functional and mature vascular formation in a rabbit ischemic model. J. Gene Med. **5**, 994–1004
8 Matsumoto, K., Okazaki, H. and Nakamura, T. (1995) Novel function of prostaglandins as inducers of gene expression of HGF and putative mediators of tissue regeneration. J. Biochem. (Tokyo) **117**, 458–464
9 Pai, R., Szabo, I. L., Soreghan, B. A., Atay, S., Kawanaka, H. and Tarnawski, A. S. (2001) PGE2 stimulates VEGF expression in endothelial cells via ERK2/JNK1 signaling pathways. Biochem. Biophys. Res. Commun. **286**, 923–928
10 Mehrabi, M. R., Serbecic, N., Tamaddon, F. et al. (2002) Clinical and experimental evidence of prostaglandin E1-induced angiogenesis in the myocardium of patients with ischemic heart disease. Cardiovasc. Res. **56**, 214–224
11 Makino, H., Aoki, M., Hashiya, N. et al. (2004) Increase in peripheral blood flow by intravenous administration of prostaglandin E1 in patients with peripheral arterial disease, accompanied by up-regulation of hepatocyte growth factor. Hypertens. Res. **27**, 85–91
12 Matsumoto, K., Morishita, R., Tomita, N. et al. (2002) Impaired endothelial dysfunction in diabetes mellitus rats was restored by oral administration of prostaglandin I2 analogue. J. Endocrinol. **175**, 217–223
13 Coker, S. J., Parratt, J. R., Ledingham, I. M. and Zeitlin, I. J. (1981) Thromboxane and prostacyclin release from ischaemic myocardium in relation to arrhythmias. Nature **291**, 323–324
14 Johnson, III, G., Furlan, L. E., Aoki, N. and Lefer, A. M. (1990) Endothelium and myocardial protecting actions of taprostene, a stable prostacyclin analogue, after acute myocardial ischemia and reperfusion in cats. Circ. Res. **66**, 1362–1370
15 de Deckere, E. A., Nugteren, D. H. and Ten Hoor, F. (1977) Prostacyclin is the major prostaglandin released from the isolated perfused rabbit and rat heart. Nature **268**, 160–163
16 Pola, R., Gaetani, E., Flex, A. et al. (2004) Comparative analysis of the *in vivo* angiogenic properties of stable prostacyclin analogs: a possible role for peroxisome proliferator-activated receptors. J. Mol. Cell. Cardiol. **36**, 363–370
17 Hayashi, K., Nagamatsu, T., Oka, T. and Suzuki, Y. (1997) Modulation of anti-glomerular basement membrane nephritis in rats by ONO-1301, a non-prostanoid prostaglandin I2 mimetic compound with inhibitory activity against thromboxane A2 synthase. Jpn J. Pharmacol. **73**, 73–82

18 Rudd, J. A., Qian, Y., Tsui, K. K. and Jones, R. L. (2000) Non-prostanoid prostacyclin mimetics as neuronal stimulants in the rat: comparison of vagus nerve and NANC innervation of the colon. Br. J. Pharmacol. **129**, 782–790
19 Murakami, S., Nagaya, N., Itoh, T. et al. (2006) Prostacyclin agonist with thromboxane synthase inhibitory activity (ONO-1301) attenuates bleomycin-induced pulmonary fibrosis in mice. Am. J. Physiol. Lung Cell. Mol. Physiol. **290**, L59–L65
20 Imawaka, H. and Sugiyama, Y. (1998) Kinetic study of the hepatobiliary transport of a new prostaglandin receptor agonist. J. Pharmacol. Exp. Ther. **284**, 949–957
21 Shiomi, T., Tsutsui, H., Hayashidani, S. et al. (2002) Pioglitazone, a peroxisome proliferator-activated receptor-γ agonist, attenuates left ventricular remodeling and failure after experimental myocardial infarction. Circulation **106**, 3126–3132
22 Bishop, E. T., Bell, G. T., Bloor, S., Broom, I. J., Hendry, N. F. and Wheatley, D. N. (1999) An *in vitro* model of angiogenesis: basic features. Angiogenesis **3**, 335–344
23 Cao, B., Su, Y., Oskarsson, M. et al. (2001) Neutralizing monoclonal antibodies to hepatocyte growth factor/scatter factor (HGF/SF) display antitumor activity in animal models. Proc. Natl. Acad. Sci. U.S.A. **98**, 7443–7448
24 Stiffey-Wilusz, J., Boice, J. A., Ronan, J., Fletcher, A. M. and Anderson, M. S. (2001) An *ex vivo* angiogenesis assay utilizing commercial porcine carotid artery: modification of the rat aortic ring assay. Angiogenesis **4**, 3–9
25 Michael, L. H., Entman, M. L., Hartley, C. J. et al. (1995) Myocardial ischemia and reperfusion: a murine model. Am. J. Physiol. Heart Circ. Physiol. **269**, H2147–H2154
26 Tanaka, K., Sata, M., Hirata, Y. and Nagai, R. (2003) Diverse contribution of bone marrow cells to neointimal hyperplasia after mechanical vascular injuries. Circ. Res. **93**, 783–790
27 Youn, H. J., Rokosh, G., Lester, S. J., Simpson, P., Schiller, N. B. and Foster, E. (1999) Two-dimensional echocardiography with a 15-MHz transducer is a promising alternative for *in vivo* measurement of left ventricular mass in mice. J. Am. Soc. Echocardiogr. **12**, 70–75
28 Sata, M., Nishimatsu, H., Suzuki, E. et al. (2001) Endothelial nitric oxide synthase is essential for the HMG-CoA reductase inhibitor cerivastatin to promote collateral growth in response to ischemia. FASEB J. **15**, 2530–2532
29 Scherrer-Crosbie, M., Ullrich, R., Bloch, K. D. et al. (2001) Endothelial nitric oxide synthase limits left ventricular remodeling after myocardial infarction in mice. Circulation **104**, 1286–1291
30 Barandon, L., Couffinhal, T., Ezan, J. et al. (2003) Reduction of infarct size and prevention of cardiac rupture in transgenic mice overexpressing FrzA. Circulation **108**, 2282–2289
31 Shoji, M., Sata, M., Fukuda, D. et al. (2004) Temporal and spatial characterization of cellular constituents during neointimal hyperplasia after vascular injury: Potential contribution of bone-marrow-derived progenitors to arterial remodeling. Cardiovasc. Pathol. **13**, 306–312
32 Nakano, N., Morishita, R., Moriguchi, A. et al. (1998) Negative regulation of local hepatocyte growth factor expression by angiotensin II and transforming growth factor-β in blood vessels: potential role of HGF in cardiovascular disease. Hypertension **32**, 444–451
33 Lee, R. J., Springer, M. L., Blanco-Bose, W. E., Shaw, R., Ursell, P. C. and Blau, H. M. (2000) VEGF gene delivery to myocardium: deleterious effects of unregulated expression. Circulation **102**, 898–901
34 Carmeliet, P. (2000) VEGF gene therapy: stimulating angiogenesis or angioma-genesis? Nat. Med. **6**, 1102–1103
35 Thurston, G., Suri, C., Smith, K. et al. (1999) Leakage-resistant blood vessels in mice transgenically overexpressing angiopoietin-1. Science **286**, 2511–2514
36 Murohara, T., Ikeda, H., Duan, J. et al. (2000) Transplanted cord blood-derived endothelial precursor cells augment postnatal neovascularization. J. Clin. Invest. **105**, 1527–1536
37 Kalka, C., Masuda, H., Takahashi, T. T. et al. (2000) Transplantation of *ex vivo* expanded endothelial progenitor cells for therapeutic neovascularization. Proc. Natl. Acad. Sci. U.S.A. **97**, 3422–3427
38 Urbich, C. and Dimmeler, S. (2004) Endothelial progenitor cells: characterization and role in vascular biology. Circ. Res. **95**, 343–353
39 Tateno, K., Minamino, T., Toko, H. et al. (2006) Critical roles of muscle-secreted angiogenic factors in therapeutic neovascularization. Circ. Res. **98**, 1194–1202
40 Morishita, R., Nakamura, S., Nakamura, Y. et al. (1997) Potential role of an endothelium-specific growth factor, hepatocyte growth factor, on endothelial damage in diabetes. Diabetes **46**, 138–142
41 Matsunaga, T., Gohda, E., Takebe, T. et al. (1994) Expression of hepatocyte growth factor is up-regulated through activation of a cAMP-mediated pathway. Exp. Cell Res. **210**, 326–335
42 Van Belle, E., Witzenbichler, B., Chen, D. et al. (1998) Potentiated angiogenic effect of scatter factor/hepatocyte growth factor via induction of vascular endothelial growth factor: the case for paracrine amplification of angiogenesis. Circulation **97**, 381–390
43 Xin, X., Yang, S., Ingle, G. et al. (2001) Hepatocyte growth factor enhances vascular endothelial growth factor-induced angiogenesis *in vitro* and *in vivo*. Am. J. Pathol. **158**, 1111–1120
44 Gille, J., Khalik, M., Konig, V. and Kaufmann, R. (1998) Hepatocyte growth factor/scatter factor (HGF/SF) induces vascular permeability factor (VPF/VEGF) expression by cultured keratinocytes. J. Invest. Dermatol. **111**, 1160–1165
45 Sakurai, S., Alam, S., Pagan-Mercado, G. et al. (2002) Retinal capillary pericyte proliferation and c-Fos mRNA induction by prostaglandin D2 through the cAMP response element. Invest. Ophthalmol. Vis. Sci. **43**, 2774–2781
46 Skrinska, V. A., Lucas, F. V., Chisolm, G. M. and Hesse, B. L. (1986) Intravenous administration of prostacyclin in rabbits: elimination kinetics and blood pressure response. J. Lab. Clin. Med. **107**, 187–193
47 Hayashi, S., Morishita, R., Nakamura, S. et al. (1999) Potential role of hepatocyte growth factor, a novel angiogenic growth factor, in peripheral arterial disease: downregulation of HGF in response to hypoxia in vascular cells. Circulation **100**, II301–II308

Received 24 October 2006/26 January 2007; accepted 31 January 2007
Published as Immediate Publication 31 January 2007, doi:10.1042/CS20060301

nature medicine

The role of autophagy in cardiomyocytes in the basal state and in response to hemodynamic stress

Atsuko Nakai[1,7], Osamu Yamaguchi[1,7], Toshihiro Takeda[1], Yoshiharu Higuchi[1], Shungo Hikoso[1], Masayuki Taniike[1], Shigemiki Omiya[1], Isamu Mizote[1], Yasushi Matsumura[2], Michio Asahi[3], Kazuhiko Nishida[1], Masatsugu Hori[1], Noboru Mizushima[4–6] & Kinya Otsu[1]

Autophagy, an evolutionarily conserved process for the bulk degradation of cytoplasmic components, serves as a cell survival mechanism in starving cells[1,2]. Although altered autophagy has been observed in various heart diseases, including cardiac hypertrophy[3,4] and heart failure[5,6], it remains unclear whether autophagy plays a beneficial or detrimental role in the heart. Here, we report that the cardiac-specific loss of autophagy causes cardiomyopathy in mice. In adult mice, temporally controlled cardiac-specific deficiency of Atg5 (autophagy-related 5), a protein required for autophagy, led to cardiac hypertrophy, left ventricular dilatation and contractile dysfunction, accompanied by increased levels of ubiquitination. Furthermore, Atg5-deficient hearts showed disorganized sarcomere structure and mitochondrial misalignment and aggregation. On the other hand, cardiac-specific deficiency of Atg5 early in cardiogenesis showed no such cardiac phenotypes under baseline conditions, but developed cardiac dysfunction and left ventricular dilatation one week after treatment with pressure overload. These results indicate that constitutive autophagy in the heart under baseline conditions is a homeostatic mechanism for maintaining cardiomyocyte size and global cardiac structure and function, and that upregulation of autophagy in failing hearts is an adaptive response for protecting cells from hemodynamic stress.

The autophagy and the ubiquitin-proteasome pathways are responsible for the degradation of intracellular components. In autophagy, cytoplasmic proteins and dysfunctional organelles are sequestered in an autophagosome, a double-membrane vesicle, delivered to the lysosome by fusion and then degraded[1,2]. The principal role of autophagy is to supply nutrients for survival[7,8]. In addition, a low level of constitutive autophagy is also important for controlling the quality of proteins and organelles, in order to maintain cell function[9,10]. Thus, autophagy functions as a cell-protective mechanism. However, autophagy also has a causative role in cell death[11]: autophagic structures are present in dying cells in neurodegenerative diseases, myopathies and liver injury[1].

Autophagic vacuoles are found in cardiomyocytes in ischemic hearts[12,13], and in human[5] and hamster[6] cardiomyopathic failing hearts. Mice with a deficiency of lysosome-associated membrane protein-2, a model for Danon disease, show an accumulation of autophagic vacuoles and cardiomyopathy[14,15]. Moreover, inhibition of autophagy has been reported in the progression of cardiac hypertrophy[3,4]. The precise role of autophagy in the heart, however, remains to be elucidated.

To determine first the role of basal constitutive autophagy in adult mouse hearts, we generated temporally controlled cardiac-specific Atg5-deficient mice. We crossed mice bearing an $Atg5^{flox}$ allele[9] with transgenic mice (*MerCreMer*) which express the *Cre* recombinase in a tamoxifen-inducible and cardiomyocyte-specific manner[16]. The resulting $Atg5^{flox/flox}$;*MerCreMer*$^{+}$ mice were indistinguishable in appearance from age-matched control $Atg5^{flox/flox}$;*MerCreMer*$^{-}$ littermates. In $Atg5^{flox/flox}$;*MerCreMer*$^{+}$ mice that had been treated with tamoxifen for 7 d, we observed an approximately 70% reduction in Atg5 protein levels in whole heart homogenates (**Fig. 1a**) and an approximately 90% reduction of Atg5 protein levels in a partially purified adult cardiomyocyte preparation (**Fig. 1b**). Successful recombination occurred 3 d after tamoxifen injection (**Fig. 1c**). Suppression of Atg5-dependent conversion of microtubule-associated protein 1 light chain 3 (LC3)-I to LC3-II (a phosphatidylethanolamine conjugate)[17,18] and accumulation of the p62/sequestosome[19] indicated a reduction in autophagy levels in tamoxifen-treated $Atg5^{flox/flox}$;*MerCreMer*$^{+}$ hearts (**Fig. 1d**). Echocardiographic analysis of tamoxifen-treated $Atg5^{flox/flox}$;*MerCreMer*$^{+}$ demonstrated left ventricular dilatation and severe contractile dysfunction (**Fig. 1e,f**). The heart-to-body and lung-to-body weight ratios were increased in tamoxifen-treated $Atg5^{flox/flox}$;*MerCreMer*$^{+}$ mice (**Fig. 1f**). Atg5-deficient hearts exhibited no abnormal histological findings; that is, no myofibrillar disarray, vacuole formation or enhanced intermuscular fibrosis, but did show an increase in the cross-sectional area of cardiomyocytes (**Fig. 2a–c**). We observed typical changes in the

[1]Department of Cardiovascular Medicine, [2]Department of Medical Information Science and [3]Department of Biochemistry, Osaka University Graduate School of Medicine, 2-2 Yamadaoka, Suita Osaka 565-0871, Japan. [4]Department of Bioregulation and Metabolism, Tokyo Metropolitan Institute of Medical Science, Bunkyoku, Tokyo 113-8613, Japan. [5]Department of Physiology and Cell Biology, Tokyo Medical and Dental University, Bunkyoku, Tokyo 113-8519, Japan. [6]Solution-Oriented Research for Science and Technology, Japan Science and Technology Agency, 4-1-8 Honmachi, Kawaguchi, Saitama 332-0012, Japan. [7]These authors contributed equally to this work. Correspondence should be addressed to K.O. (kotsu@medone.med.osaka-u.ac.jp).

Received 10 November 2006; accepted 7 March 2007; published online 22 April 2007; doi:10.1038/nm1574

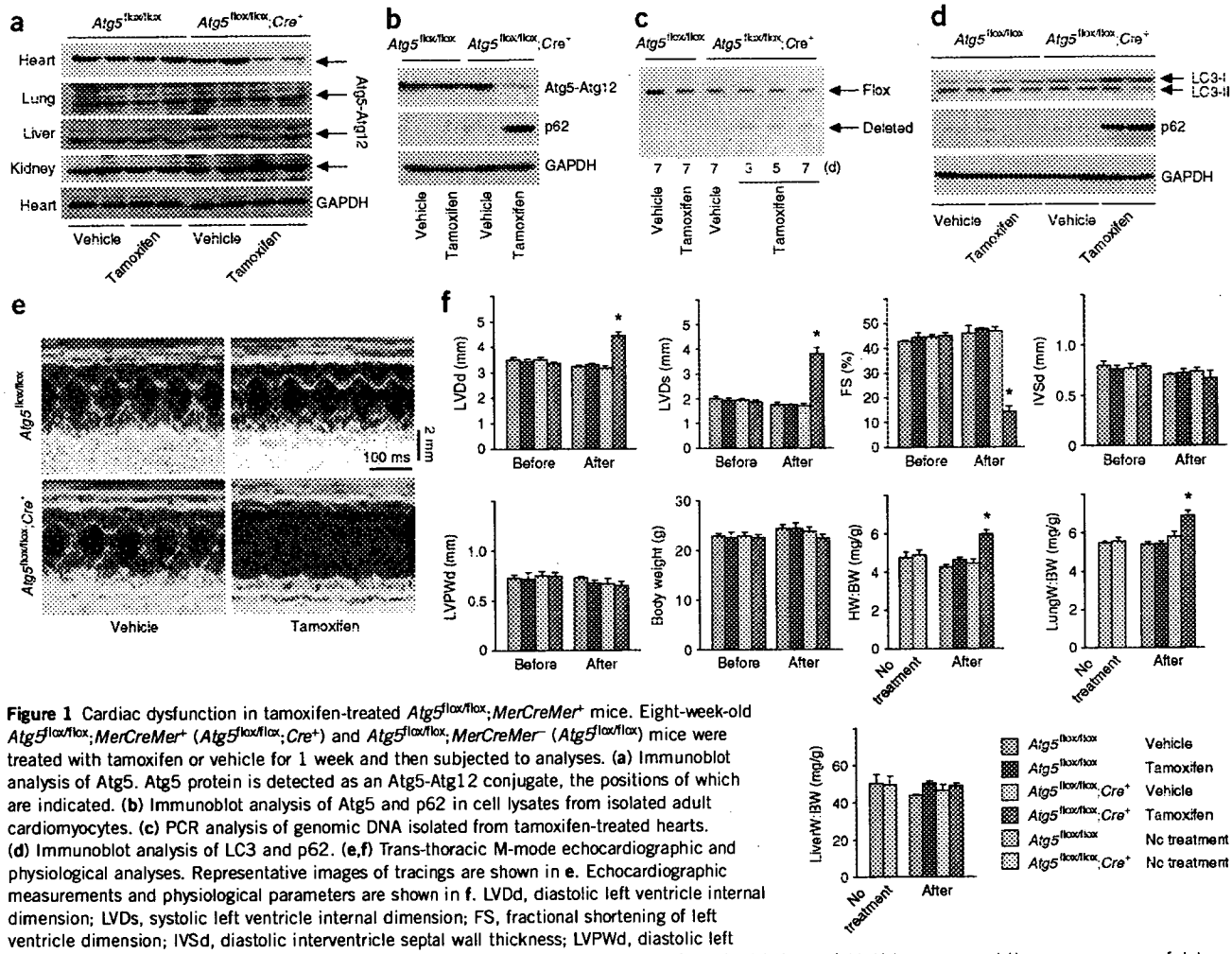

Figure 1 Cardiac dysfunction in tamoxifen-treated *Atg5*$^{flox/flox}$;*MerCreMer*$^{+}$ mice. Eight-week-old *Atg5*$^{flox/flox}$;*MerCreMer*$^{+}$ (*Atg5*$^{flox/flox}$;*Cre*$^{+}$) and *Atg5*$^{flox/flox}$;*MerCreMer*$^{-}$ (*Atg5*$^{flox/flox}$) mice were treated with tamoxifen or vehicle for 1 week and then subjected to analyses. (**a**) Immunoblot analysis of Atg5. Atg5 protein is detected as an Atg5-Atg12 conjugate, the positions of which are indicated. (**b**) Immunoblot analysis of Atg5 and p62 in cell lysates from isolated adult cardiomyocytes. (**c**) PCR analysis of genomic DNA isolated from tamoxifen-treated hearts. (**d**) Immunoblot analysis of LC3 and p62. (**e,f**) Trans-thoracic M-mode echocardiographic and physiological analyses. Representative images of tracings are shown in **e**. Echocardiographic measurements and physiological parameters are shown in **f**. LVDd, diastolic left ventricle internal dimension; LVDs, systolic left ventricle internal dimension; FS, fractional shortening of left ventricle dimension; IVSd, diastolic interventricle septal wall thickness; LVPWd, diastolic left ventricle posterior wall thickness; BW, body weight; HW, heart weight; lungW, lung weight; liverW, liver weight. Values represent the mean ± s.e.m. of data from 3 to 8 mice in each group. Echocardiographic and body weight measurements were performed sequentially before and after treatment. $^{*}P < 0.05$ versus all other groups.

mRNA expression of molecular markers for cardiac remodeling in Atg5-deficient hearts, such as increased levels of atrial natriuretic factor (*Nppa*) and brain natriuretic peptide (*Nppb*) mRNAs and decreased levels of sarco(endo)plasmic reticulum Ca^{2+}-ATPase (*Serca2a*, also known as *Atp2a2*) and phospholamban (*Pln*) mRNAs (**Fig. 2d**). The protein levels of SERCA2a and phospholamban decreased in parallel with changes in their mRNA levels (**Fig. 2e**). Measurements of intracellular Ca^{2+} transients indicated impaired Ca^{2+} cycling in isolated Atg5-deficient cardiomyocytes (**Fig. 2f**) (peak amplitude of Ca^{2+} transient: 0.38 ± 0.01 in vehicle-treated *Atg5*$^{flox/flox}$;*MerCreMer*$^{+}$ versus 0.29 ± 0.03 in tamoxifen-treated *Atg5*$^{flox/flox}$;*MerCreMer*$^{+}$; half-decay time: 0.165 ± 0.006 s in vehicle-treated *Atg5*$^{flox/flox}$;*MerCreMer*$^{+}$ versus 0.714 ± 0.103 s in tamoxifen-treated *Atg5*$^{flox/flox}$;*MerCreMer*$^{+}$; $n = 3$, $P < 0.05$ for each comparison). Thus, cardiac-specific reduction in autophagy in adulthood led to contractile dysfunction, heart failure and cardiac hypertrophy.

To clarify the role of autophagy in cardiomyocyte hypertrophy, we infected rat neonatal cardiomyocytes with an adenovirus expressing short hairpin RNA (shRNA) targeted to *Atg7* (Ad-*Atg7*-RNAi), encoding the protein Atg7 which is essential for autophagosome formation[1], or control nonspecific shRNA (Ad-ns-RNAi). As only a small amount of Atg5 is needed for autophagy[20], knockdown of *Atg5* to levels low enough to block autophagy might be difficult to achieve, and we chose to knockdown *Atg7* instead. Ad-*Atg7*-RNAi reduced Atg7 protein levels and inhibited autophagy, as evidenced by a decrease in LC3-II protein levels and an accumulation of p62 (**Supplementary Fig. 1** online). Ad-*Atg7*-RNAi induced the morphological and biochemical features of *in vitro* cardiomyocyte hypertrophy (**Supplementary Fig. 1**). Thus, inhibition of autophagy induces cardiomyocyte hypertrophy with typical characteristics.

Polyubiquitinated protein levels and proteasome activity increased in tamoxifen-treated *Atg5*$^{flox/flox}$;*MerCreMer*$^{+}$ hearts (**Fig. 3a,b**). Ultrastructural analyses of *Atg5*-deficient hearts revealed a disorganized sarcomere structure, misalignment and aggregation of mitochondria, and aberrant concentric membranous structures similar to those observed in *Atg7*-deficient livers[8] (**Fig. 3c**), suggesting the importance of autophagy in the turnover of organelles. We observed increased activation of S6 kinase in Atg5-deficient hearts (**Fig. 3a**), suggestive of enhanced protein synthesis, which may also contribute to the cardiac hypertrophy observed.

The accumulation of ubiquitinated proteins is known to induce endoplasmic reticulum stress. GRP78 and GRP94 protein levels were

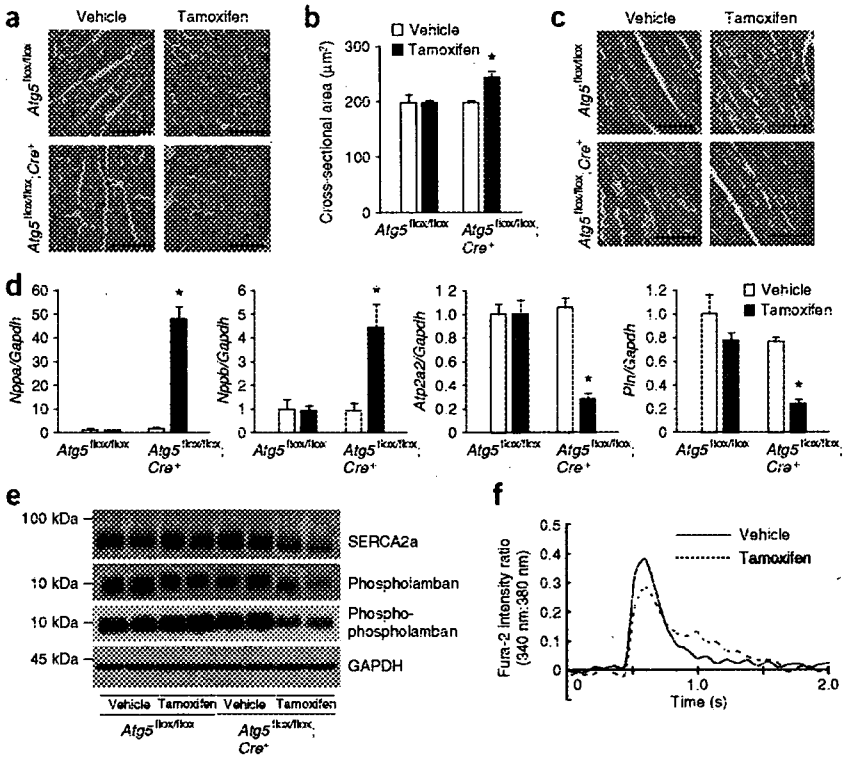

Figure 2 Hypertrophic responses in tamoxifen-treated *Atg5*$^{flox/flox}$;*MerCreMer*$^{+}$ mice. *Atg5*$^{flox/flox}$;*MerCreMer*$^{+}$ (*Atg5*$^{flox/flox}$;*Cre*$^{+}$) and *Atg5*$^{flox/flox}$;*MerCreMer*$^{-}$ (*Atg5*$^{flox/flox}$) mice were treated with tamoxifen or vehicle for 1 week and then subjected to analyses. **(a)** H&E-stained sections of left ventricle. **(b)** Cross-sectional area of cardiomyocytes. Values represent the mean ± s.e.m. of data from 3 to 8 mice in each group. **(c)** Mallory-Azan–stained sections of left ventricle. **(d)** Effect of *Atg5* deficiency on *Nppa*, *Nppb*, *Atp2a2* and *Pln* mRNA expression. mRNA levels were determined by quantitative RT-PCR. Data were normalized to the *Gapdh* content and are expressed as fold increase over levels in vehicle-treated *Atg5*$^{flox/flox}$ groups. Values represent the mean ± s.e.m. of data from 5 to 7 mice in each group. **(e)** Immunoblot analysis of SERCA2a, total phospholamban and phospho-phospholamban. **(f)** Representative calcium transients of isolated cardiomyocytes from *Atg5*$^{flox/flox}$;*Cre*$^{+}$ hearts treated with tamoxifen or vehicle. The fluorescence emission is expressed as the ratio of the signals obtained with excitation at 340 and 380 nm wavelengths. Fluorescent signals from 10 to 20 cardiomyocytes from one mouse in each group were averaged. Scale bars, 50 μm. *$P < 0.05$ versus all other groups.

markedly increased in Atg5-deficient hearts (**Fig. 3d**). The abundance of cleaved caspase-12, which mediates the endoplasmic reticulum–specific apoptotic pathway[21], and the number of TUNEL-positive cells, identified as cardiomyocytes by α-sarcomeric actin staining, was significantly increased in Atg5-deficient hearts (**Fig. 3e,f**). Ad-*Atg7*-RNAi reduced the viable cell number and increased levels of cleaved caspase-12 *in vitro* (**Supplementary Fig. 1**).

This inverse correlation between the extent of autophagy and apoptosis is in agreement with a previous report that the inactivation of autophagy triggers apoptosis[22]. Our findings indicate that autophagy mediates the essential and continuous turnover of intracellular proteins and organelles in the heart. The downregulation of protein turnover could cause abnormal proteins to accumulate, promoting endoplasmic reticulum stress, leading to apoptosis and cardiac dysfunction. As there was no histological evidence of substantial myocyte loss or replacement fibrosis in Atg5-deficient hearts, mechanisms in addition to apoptosis seem to be involved in the pathogenesis of the drastic cardiac dysfunction observed. Deficiency of Atg5 or Atg7 in neural cells led to progressive deficits in motor function, associated with increased levels of ubiquitinated protein[9,10]. It is also possible that the accumulation of abnormal proteins or organelles may directly cause cardiac dysfunction. Basal autophagy is a homeostatic mechanism for the maintenance of normal cardiac function and morphology.

We next attempted to confirm these observations using another line of cardiac-specific Atg5-deficient mice, in which *Atg5* was deleted during cardiogenesis. We crossed *Atg5*^{flox} mice with knock-in mice expressing *Cre* under the control of myosin light chain 2v (MLC2v) promoter[23], to produce *Atg5*$^{flox/flox}$;MLC2v-*Cre*$^{+}$ mice. In these mice, *Cre* is expressed in cardiomyocytes after embryonic day 8 (ref. 23). We used *Atg5*$^{flox/flox}$;MLC2v-*Cre*$^{-}$ littermates as controls. PCR analysis of genomic DNA isolated from *Atg5*$^{flox/flox}$;MLC2v-*Cre*$^{+}$ hearts indicated successful recombination (**Supplementary Fig. 2** online). In contrast to tamoxifen-treated *Atg5*$^{flox/flox}$;*MerCreMer*$^{+}$ mice, Atg5$^{flox/flox}$;MLC2v-*Cre*$^{+}$ mice showed no cardiac hypertrophy or dysfunction, suggesting that compensatory mechanisms are able to prevent pathological consequences of autophagy inhibition from occurring (**Supplementary Fig. 2**). We also used *Atg5*-deficient mice in which *Cre* is expressed under control of the α-myosin heavy chain (α-MyHC) promoter on a C57BL/6 background[24]. The α-MyHC promoter becomes active in cardiomyocytes between embryonic day 7.5 and 8 (ref. 25). The resulting mice exhibited no cardiac abnormalities (**Supplementary Fig. 3** online), thus excluding the possibility that the genetic background or the specific constructs used were responsible for the phenotypic differences observed in inducible versus constitutive Atg5-deficient mice. In *Atg5*$^{flox/flox}$;MLC2v-*Cre*$^{+}$ mice, the reduction in autophagy may be too acute for compensatory mechanisms to be effective.

We then sought to clarify the role of autophagy in response to stress such as pressure overload. In wild-type mice, pressure overload by means of a thoracic transverse aortic constriction (TAC) induced cardiac hypertrophy 1 week after the operation and heart failure 4 weeks after the operation[26]. Although autophagy was suppressed in TAC-induced hypertrophied hearts at the 1 week time point, as indicated by decreased LC3-II levels, it was upregulated in failing hearts at the 4 week time point, as indicated by increased LC3-II levels (**Supplementary Fig. 4** online). These alterations in autophagy are in agreement with previous reports[4–7].

To elucidate the role of autophagy in cardiac remodeling, we performed TAC operations on *Atg5*$^{flox/flox}$;MLC2v-*Cre*$^{+}$ mice. Autophagy was suppressed in sham- and TAC-operated *Atg5*$^{flox/flox}$;MLC2v-*Cre*$^{+}$ hearts compared to the corresponding controls (**Fig. 4a**). The *Atg5*$^{flox/flox}$;MLC2v-*Cre*$^{+}$ mice showed severe cardiac dysfunction and left ventricular dilatation 1 week after TAC (**Fig. 4b,c**) and died of heart failure thereafter. Pressure overload activated S6

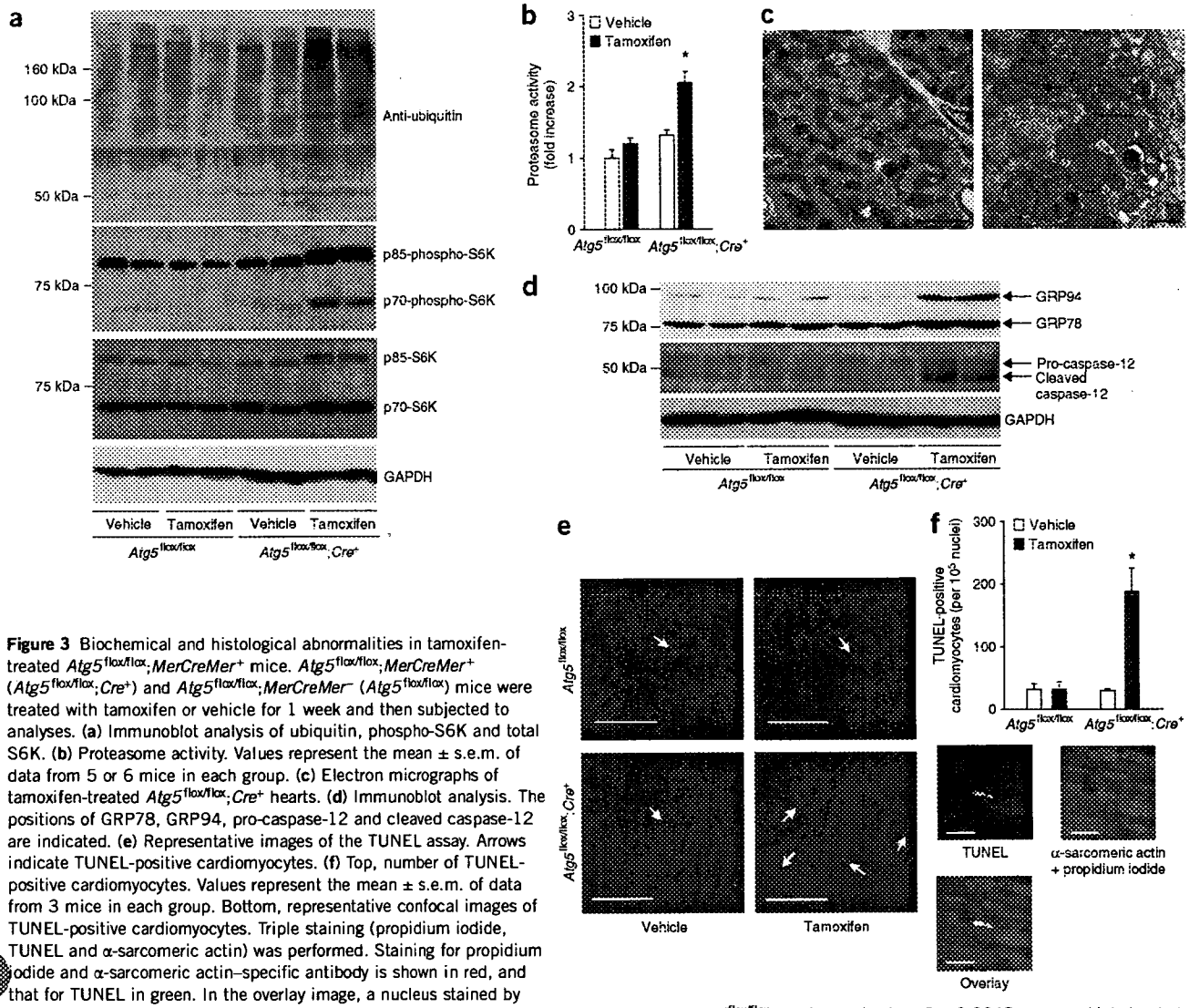

Figure 3 Biochemical and histological abnormalities in tamoxifen-treated *Atg5*$^{flox/flox}$;*MerCreMer*$^{+}$ mice. *Atg5*$^{flox/flox}$;*MerCreMer*$^{+}$ (*Atg5*$^{flox/flox}$;*Cre*$^{+}$) and *Atg5*$^{flox/flox}$;*MerCreMer*$^{-}$ (*Atg5*$^{flox/flox}$) mice were treated with tamoxifen or vehicle for 1 week and then subjected to analyses. (**a**) Immunoblot analysis of ubiquitin, phospho-S6K and total S6K. (**b**) Proteasome activity. Values represent the mean ± s.e.m. of data from 5 or 6 mice in each group. (**c**) Electron micrographs of tamoxifen-treated *Atg5*$^{flox/flox}$;*Cre*$^{+}$ hearts. (**d**) Immunoblot analysis. The positions of GRP78, GRP94, pro-caspase-12 and cleaved caspase-12 are indicated. (**e**) Representative images of the TUNEL assay. Arrows indicate TUNEL-positive cardiomyocytes. (**f**) Top, number of TUNEL-positive cardiomyocytes. Values represent the mean ± s.e.m. of data from 3 mice in each group. Bottom, representative confocal images of TUNEL-positive cardiomyocytes. Triple staining (propidium iodide, TUNEL and α-sarcomeric actin) was performed. Staining for propidium iodide and α-sarcomeric actin–specific antibody is shown in red, and that for TUNEL in green. In the overlay image, a nucleus stained by both TUNEL and propidium iodide is shown in yellow. In comparison to tamoxifen-treated *Atg5*$^{flox/flox}$;*MerCreMer*$^{+}$ mice, $P = 0.0048$ versus vehicle-treated *Atg5*$^{flox/flox}$;*MerCreMer*$^{-}$, $P = 0.0049$ versus tamoxifen-treated *Atg5*$^{flox/flox}$;*MerCreMer*$^{-}$, $P = 0.0046$ versus vehicle-treated *Atg5*$^{flox/flox}$;*MerCreMer*$^{+}$. *$P < 0.05$ versus all other groups. Scale bars: 5 μm in **c** left, 1 μm in **c** right; 100 μm in **e**; 20 μm in **f**.

kinase in the heart, but its activation was greater in TAC-operated *Atg5*$^{flox/flox}$;MLC2v-*Cre*$^{+}$ mice than in controls (**Fig. 4d**). Polyubiquitinated protein, GRP94 and GRP78 levels were markedly increased in TAC-operated *Atg5*$^{flox/flox}$;MLC2v-*Cre*$^{+}$ hearts in comparison to controls (**Fig. 4e**). After TAC, proteasome activity in *Atg5*$^{flox/flox}$;MLC2v-*Cre*$^{+}$ hearts was higher than that in controls (**Fig. 4f**). These findings suggest that reduced autophagy resulted in the enhancement of both protein synthesis and proteasome-dependent protein degradation in pressure-overloaded hearts. The number of TUNEL-positive cardiomyocytes increased in *Atg5*$^{flox/flox}$;MLC2v-*Cre*$^{+}$ hearts after TAC (**Fig. 4g**). The heart-to-body weight ratio and cardiomyocyte cross-sectional area increased to a similar degree in *Atg5*$^{flox/flox}$;MLC2v-*Cre*$^{+}$ and controls after TAC (**Fig. 4h**), suggesting that autophagy does not play a role in regulating the cardiomyocyte hypertrophy induced by pressure overload or that its function in the hypertrophic process is compensated by the action of other hypertrophic signaling mechanisms. TAC in both groups induced typical changes in molecular markers indicative of cardiac remodeling (**Supplementary Fig. 5** online).

We next examined the effect of autophagy inhibition on β-adrenergic stress–induced cell death in the heart. Infusion of isoproterenol for 7 d in *Atg5*$^{flox/flox}$;MLC2v-*Cre*$^{+}$ led to left ventricular dilatation and contractile dysfunction compared to that in controls (**Supplementary Fig. 6** online). Furthermore, isolated adult cardiomyocytes from *Atg5*$^{flox/flox}$;MLC2v-*Cre*$^{+}$ hearts were more susceptible than cardiomyocytes isolated from control hearts to isoproterenol.

Our results indicate that autophagy plays a beneficial role in the heart in response to pressure overload or β-adrenergic stress. In particular, autophagy seems needed to increase protein turnover in remodeling hearts and may be important for preventing the accumulation of abnormal proteins or damaged organelles, which could disrupt cardiac function. In the absence of autophagy, the accumulation of polyubiquitinated proteins may be responsible for increased endoplasmic reticulum stress, resulting in apoptosis. The

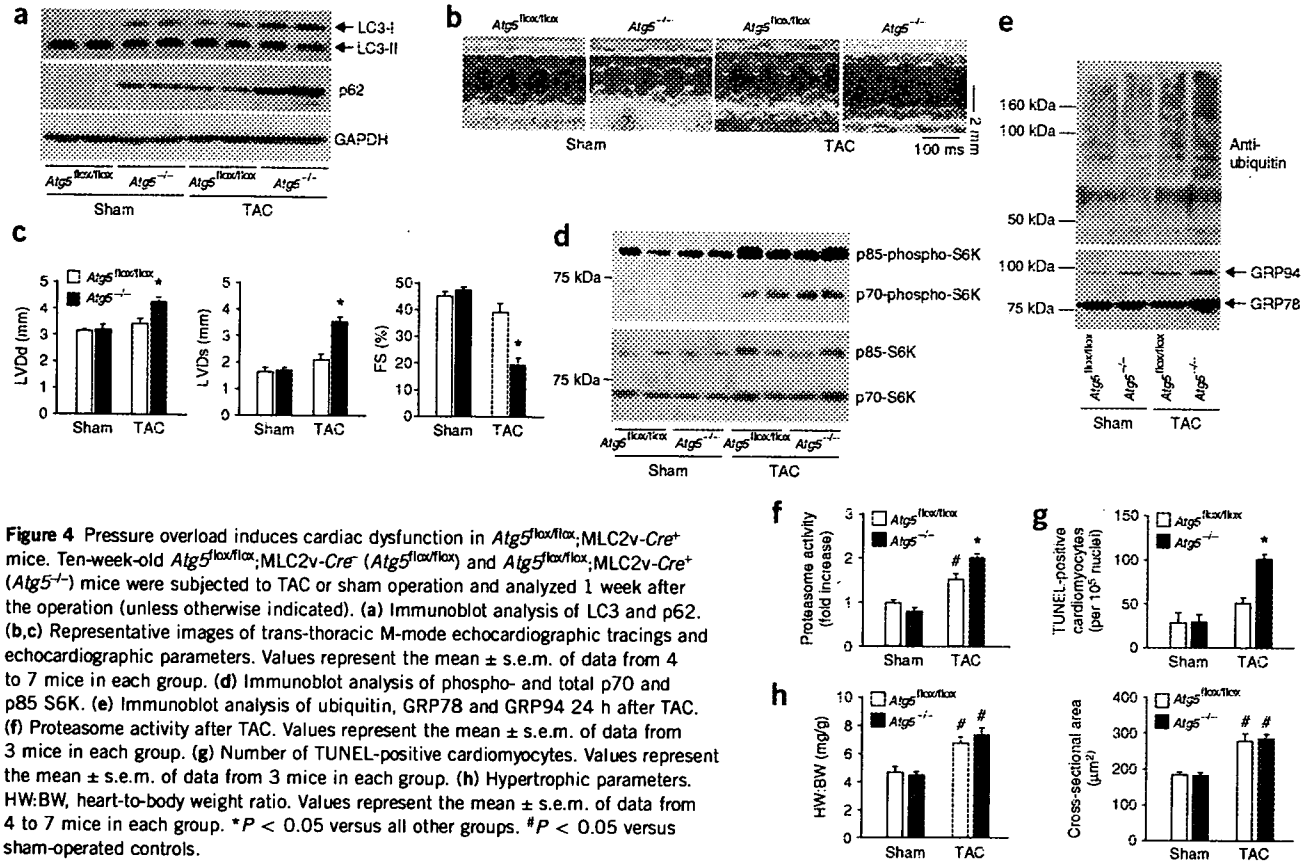

Figure 4 Pressure overload induces cardiac dysfunction in *Atg5*$^{flox/flox}$;MLC2v-*Cre*$^{+}$ mice. Ten-week-old *Atg5*$^{flox/flox}$;MLC2v-*Cre*$^{-}$ (*Atg5*$^{flox/flox}$) and *Atg5*$^{flox/flox}$;MLC2v-*Cre*$^{+}$ (*Atg5*$^{-/-}$) mice were subjected to TAC or sham operation and analyzed 1 week after the operation (unless otherwise indicated). (**a**) Immunoblot analysis of LC3 and p62. (**b**,**c**) Representative images of trans-thoracic M-mode echocardiographic tracings and echocardiographic parameters. Values represent the mean ± s.e.m. of data from 4 to 7 mice in each group. (**d**) Immunoblot analysis of phospho- and total p70 and p85 S6K. (**e**) Immunoblot analysis of ubiquitin, GRP78 and GRP94 24 h after TAC. (**f**) Proteasome activity after TAC. Values represent the mean ± s.e.m. of data from 3 mice in each group. (**g**) Number of TUNEL-positive cardiomyocytes. Values represent the mean ± s.e.m. of data from 3 mice in each group. (**h**) Hypertrophic parameters. HW:BW, heart-to-body weight ratio. Values represent the mean ± s.e.m. of data from 4 to 7 mice in each group. $^{*}P < 0.05$ versus all other groups. $^{\#}P < 0.05$ versus sham-operated controls.

level of apoptosis observed, however, seems too low for this to be a primary cause of cardiomyopathy in autophagy-deficient, pressure-overloaded hearts, as even a 15-fold increase in apoptosis resulted in only slowly progressive heart failure[27]. As autophagy is a mechanism for maintaining energy homeostasis during starvation[1,2], it is also possible that it is necessary to compensate for increased energy demand during remodeling. Autophagy may be an active adaptive intervention for protecting cardiomyocytes under stress by regulating cardiomyocyte death and function.

METHODS

Mice, and *in vivo* assessment of cardiac function. The generation of mice bearing an *Atg5*^{flox} allele, in which exon 3 of the *Atg5* gene is flanked by two *loxP* sequences, has been previously reported[9]. Mice bearing an *Atg5*^{flox} allele were crossed with transgenic α-MyHC-*MerCreMer* mice[16], MLC2v-*Cre* mice[23] or α-MyHC-*Cre* mice[24]. Genomic DNA isolated from mice bearing an *Atg5*^{flox} was subjected to PCR analysis[9]. The mice were maintained individually and allowed access to water and mouse chow *ad libitum*. We administered a subcutaneous injection of 80 μg per g (body weight) per d of 4-hydroxytamoxifen (Sigma) or vehicle to 8-week-old male mice once daily for 1 week. We performed TAC on 10-week-old male mice as previously described[26]. We used osmotic minipumps (model 1007D, Alzet) to administer isoproterenol at a dose of 7.5 mg per kg (body weight) per d for 1 week. To perform echocardiography on awake mice, we used ultra-sonography (SONOS-5500, equipped with a 15-MHz linear transducer, Philips Medical Systems), 12 h after the last tamoxifen injection or 1 week after TAC. This study was carried out under the supervision of the Animal Research Committee of Osaka University and in accordance with the Guidelines for Animal Experiments of Osaka University and the Japanese Animal Protection and Management Law (No. 25).

Neonatal cardiomyocyte culture and adenoviral infection. We prepared rat ventricular myocytes from 1- to 2-d-old Wistar rats as described elsewhere[28]. Cardiomyocytes were plated in low serum medium (Dulbecco's modified Eagle's medium containing 0.5% FBS). The cells were then incubated for 48 h, infected with adenoviral vectors expressing shRNA targeted to *Atg7* at a multiplicity of infection of 10, and incubated for an additional 48 h for experiments. We designed target-specific shRNA duplexes from the open reading frame of rat *Atg7* mRNA. The selected sequence was then submitted to a BLAST search to ensure that *Atg7* mRNA was exclusively targeted. Finally, a 70-bp shRNA fragment was inserted into the pSIREN-DNR Vector (BD knockout RNAi systems, Clontech). The negative control shRNA used was constructed using Negative Control Annealed Oligonucleotide (BD knockout RNAi systems, Clontech).

Isolation and characterization of adult mouse ventricular myocytes. We isolated mouse adult cardiomyocytes from 10-week-old male mice as previously reported[29]. The cardiomyocytes were subjected to western blotting analysis or treated with 1 μM isoproterenol for 4 h (ref. 29). We determined the number of dead cells by Trypan blue staining.

We also examined Ca^{2+} transients in cardiomyocytes using Fura-2 loading. Myocytes were placed on the stage of a Nikon TE200-U inverted confocal microscope (Nikon). The Fura-2 signal was recorded at 22–24 °C at a stimulation frequency of 0.25 Hz. The excitation wavelengths were 340 nm and 380 nm, and the fluorescence emission was detected at 505 nm; the signal is expressed as the ratio of the emissions at the two excitation wavelengths (F_{340}/F_{380}). We averaged fluorescent signals from 10 to 20 cardiomyocytes from a single heart.

Antibodies. The following antibodies were used for the immunoblot analysis: SERCA2A-specific monoclonal antibody (Santa Cruz, sc-8094), phospholamban-specific monoclonal antibody (A1) and rabbit

phospho-phospholamban–specific polyclonal antibody (Upstate, Ser16), guinea pig p62-specific (C-terminal–specific) polyclonal antibody (Progen, GP62), rabbit ubiquitin-specific polyclonal antibody (DakoCytomation, Z0458), rabbit p70 S6 kinase–specific (AF8962) and phospho-p70 S6 kinase–specific polyclonal antibodies (R&D Systems, T421/S424), monoclonal caspase-12–specific antibody (Sigma, 14F7), monoclonal KDEL-specific antibody (Stressgen Biotechnologies, SPA-827), monoclonal GAPDH-specific antibody (Abcam, ab9482), and antibodies to Atg5 (ref. 30) and LC3 (ref. 17). Tissues were lysed in a homogenization buffer (50 mM Tris-HCl, pH 7.4, 1 mM EDTA, 1 mM EGTA, 1% Triton X-100) with proteinase inhibitors[24]. Western blots were developed with the ECL Plus kit or ECL Advance kit (Amersham Biosciences Corp.). The quantification of signals was performed by densitometry of scanned autoradiographs with the aid of Scion Image software (version 4.0.2; Scion Corp.).

Histological analysis. Hearts were excised and immediately fixed in buffered 4% paraformaldehyde, embedded in paraffin, and sectioned to a thickness of 3 μm. We performed H&E or Mallory-Azan staining on serial sections. To determine the number of cells undergoing nuclear fragmentation, we performed a TUNEL assay on paraffin-embedded heart sections, using an *in situ* apoptosis detection kit (Takara Bio Inc.). For electron microscopy, the hearts were fixed with 2.5% glutaraldehyde in PBS.

Proteasome activity analysis. We evaluated proteasome activity in homogenates of hearts using a Proteasome Activity Assay Kit (Chemicon).

Quantitative real-time reverse transcriptase-PCR (RT-PCR). We isolated total RNA from the left ventricle for analysis using the TRIzol reagent (Life Technologies). We determined mRNA levels for *Nppa*, *Nppb*, *Atp2a2*, α-skeletal actin (*Acta1*) and *Pln* by quantitative RT-PCR. For reverse transcription and amplification, we used the TaqMan Reverse Transcription Reagents (PerkinElmer Life Sciences) and Platinum Quantitative PCR SuperMix-UDG (Invitrogen Life Technologies), respectively. The PCR primers and probes were obtained from PerkinElmer Life Sciences. We constructed RT-PCR standard curves using the corresponding cDNA. All data were normalized to *Gapdh* content and are expressed as fold increase over the control group.

Statistical analysis. Results are shown as the mean ± s.e.m. Paired data were evaluated by Student's *t*-test, and a one-way analysis of variance (ANOVA) was used for multiple comparisons. A value of $P < 0.05$ was considered statistically significant.

Note: Supplementary information is available on the Nature Medicine website.

ACKNOWLEDGMENTS

We are grateful to K. Chien (Harvard University) for the gift of MLC-2v *Cre* mice, J. Molkentin (Cincinnati Children's Hospital Medical Center) for *MerCreMer* mice, T. Yoshimori (Osaka University) for antibody to LC3 and E. Lakatta for teaching us to isolate adult mouse cardiomyocytes. This work was supported by a Grant-in-Aid for Scientific Research from the Ministry of Education, Culture, Sports, Science and Technology to K.O. (16590683). O.Y. held a postdoctoral fellowship from the Japan Society for the Promotion of Science. S.H. was the recipient of a postdoctoral fellowship from the Center of Excellence Research of the Ministry of Education, Culture, Sports, Science and Technology. T.T. received a postdoctoral fellowship from the Japan Health Science Foundation.

AUTHOR CONTRIBUTIONS

A.N. worked on the *in vitro* analysis of the mice; O.Y. conducted the *in vivo* analysis of the mice and wrote the manuscript; T.T. performed adult cardiomyocyte isolation and Ca^{2+} transient experiments; Y.H. performed ischemia-reperfusion surgery; S.H. assisted with RT-PCR experiments; M.T., S.O. and I.M. contributed to the *in vitro* experiments; Y.M. performed statistical analysis of the data; M.A. contributed to Ca^{2+} transient measurements; K.N. contributed to the *in vivo* experiments; M.H. supervised this project; N.M. provided advice on designing and conducting experiments; K.O. conceived, designed and directed the study.

COMPETING INTERESTS STATEMENT

The authors declare no competing financial interests.

Published online at http://www.nature.com/naturemedicine
Reprints and permissions information is available online at http://npg.nature.com/reprintsandpermissions

1. Mizushima, N., Ohsumi, Y. & Yoshimori, T. Autophagosome formation in mammalian cells. *Cell Struct. Funct.* **27**, 421–429 (2002).
2. Levine, B. & Klionsky, D.J. Development by self-digestion: molecular mechanisms and biological functions of autophagy. *Dev. Cell* **6**, 463–477 (2004).
3. Dammrich, J. & Pfeifer, U. Cardiac hypertrophy in rats after supravalvular aortic constriction. II. Inhibition of cellular autophagy in hypertrophying cardiomyocytes. *Virchows Arch. B Cell Pathol. Incl. Mol. Pathol.* **43**, 287–307 (1983).
4. Pfeifer, U., Fohr, J., Wilhelm, W. & Dammrich, J. Short-term inhibition of cardiac cellular autophagy by isoproterenol. *J. Mol. Cell. Cardiol.* **19**, 1179–1184 (1987).
5. Shimomura, H. *et al.* Autophagic degeneration as a possible mechanism of myocardial cell death in dilated cardiomyopathy. *Jpn. Circ. J.* **65**, 965–968 (2001).
6. Miyata, S. *et al.* Autophagic cardiomyocyte death in cardiomyopathic hamsters and its prevention by granulocyte colony-stimulating factor. *Am. J. Pathol.* **168**, 386–397 (2006).
7. Kuma, A. *et al.* The role of autophagy during the early neonatal starvation period. *Nature* **432**, 1032–1036 (2004).
8. Komatsu, M. *et al.* Impairment of starvation-induced and constitutive autophagy in Atg7-deficient mice. *J. Cell Biol.* **169**, 425–434 (2005).
9. Hara, T. *et al.* Suppression of basal autophagy in neural cells causes neurodegenerative disease in mice. *Nature* **441**, 885–889 (2006).
10. Komatsu, M. *et al.* Loss of autophagy in the central nervous system causes neurodegeneration in mice. *Nature* **441**, 880–884 (2006).
11. Baehrecke, E.H. Autophagy: dual roles in life and death? *Nat. Rev. Mol. Cell Biol.* **6**, 505–510 (2005).
12. Decker, R.S. & Wildenthal, K. Lysosomal alterations in hypoxic and reoxygenated hearts. I. Ultrastructural and cytochemical changes. *Am. J. Pathol.* **98**, 425–444 (1980).
13. Yan, L. *et al.* Autophagy in chronically ischemic myocardium. *Proc. Natl. Acad. Sci. USA* **102**, 13807–13812 (2005).
14. Nishino, I. *et al.* Primary LAMP-2 deficiency causes X-linked vacuolar cardiomyopathy and myopathy (Danon disease). *Nature* **406**, 906–910 (2000).
15. Tanaka, Y. *et al.* Accumulation of autophagic vacuoles and cardiomyopathy in LAMP-2-deficient mice. *Nature* **406**, 902–906 (2000).
16. Sohal, D.S. *et al.* Temporally regulated and tissue-specific gene manipulations in the adult and embryonic heart using a tamoxifen-inducible Cre protein. *Circ. Res.* **89**, 20–25 (2001).
17. Kabeya, Y. *et al.* LC3, a mammalian homologue of yeast Apg8p, is localized in autophagosome membranes after processing. *EMBO J.* **19**, 5720–5728 (2000).
18. Mizushima, N., Yamamoto, A., Matsui, M., Yoshimori, T. & Ohsumi, Y. *In vivo* analysis of autophagy in response to nutrient starvation using transgenic mice expressing a fluorescent autophagosome marker. *Mol. Biol. Cell* **15**, 1101–1111 (2004).
19. Bjorkoy, G. *et al.* p62/SQSTM1 forms protein aggregates degraded by autophagy and has a protective effect on huntingtin-induced cell death. *J. Cell Biol.* **171**, 603–614 (2005).
20. Hosokawa, N., Hara, Y. & Mizushima, N. Generation of cell lines with tetracycline-regulated autophagy and a role for autophagy in controlling cell size. *FEBS Lett.* **580**, 2623–2629 (2006).
21. Nakagawa, T. *et al.* Caspase-12 mediates endoplasmic-reticulum-specific apoptosis and cytotoxicity by amyloid-beta. *Nature* **403**, 98–103 (2000).
22. Boya, P. *et al.* Inhibition of macroautophagy triggers apoptosis. *Mol. Cell. Biol.* **25**, 1025–1040 (2005).
23. Chen, J. *et al.* Selective requirement of myosin light chain 2v in embryonic heart function. *J. Biol. Chem.* **273**, 1252–1256 (1998).
24. Yamaguchi, O. *et al.* Cardiac-specific disruption of the c-raf-1 gene induces cardiac dysfunction and apoptosis. *J. Clin. Invest.* **114**, 937–943 (2004).
25. Lyons, G.E. *et al.* Developmental regulation of myosin gene expression in mouse cardiac muscle. *J. Cell Biol.* **111**, 2427–2436 (1990).
26. Yamaguchi, O. *et al.* Targeted deletion of apoptosis signal-regulating kinase 1 attenuates left ventricular remodeling. *Proc. Natl. Acad. Sci. USA* **100**, 15883–15888 (2003).
27. Wencker, D. *et al.* A mechanistic role for cardiac myocyte apoptosis in heart failure. *J. Clin. Invest.* **111**, 1497–1504 (2003).
28. Hirotani, S. *et al.* Involvement of nuclear factor-κB and apoptosis signal-regulating kinase 1 in G-protein-coupled receptor agonist-induced cardiomyocyte hypertrophy. *Circulation* **105**, 509–515 (2002).
29. Zhou, Y.Y. *et al.* Culture and adenoviral infection of adult mouse cardiac myocytes: methods for cellular genetic physiology. *Am. J. Physiol. Heart Circ. Physiol.* **279**, H429–H436 (2000).
30. Mizushima, N. *et al.* Dissection of autophagosome formation using Apg5-deficient mouse embryonic stem cells. *J. Cell Biol.* **152**, 657–668 (2001).

Reprinted from HEART, June 2007, Vol 93, p 711-715

HEART FAILURE AND CARDIOMYOPATHY

Prognosis and prognostic factors in patients with hypertrophic cardiomyopathy in Japan: results from a nationwide study

Ali Nasermoaddeli, Katsuyuki Miura, Akira Matsumori, Yoshiyuki Soyama, Yuko Morikawa, Akira Kitabatake, Yutaka Inaba, Hideaki Nakagawa

Heart 2007;**93**:711–715. doi: 10.1136/hrt.2006.095232

See end of article for authors' affiliations

Correspondence to: Dr K Miura, Department of Epidemiology and Public Health, Kanazawa Medical University, 1–1 Daigaku, Uchinada, Ishikawa 920–0293, Japan; miura@kanazawa-med.ac.jp

Accepted 26 September 2006
Published Online First 3 November 2006

Objective: To investigate prognosis and prognostic factors in patients with hypertrophic cardiomyopathy (HCM) in Japan.
Design: A nationwide epidemiological study.
Setting: Hospitals selected randomly from among all hospitals in Japan.
Patients: Clinical and epidemiological information for 2155 patients with HCM were collected in 1999.
Main outcome measures: Patients were classified on the basis of baseline prognostic factors. Survival rates up to 5 years were calculated by Cox's proportional hazard model for 1605 patients.
Results: During the follow-up period, 241 deaths were recorded. The crude 5-year survival rate for the entire cohort was 86% (95% CI 84 to 88), and annual mortality ranged from 2.2% to 3.0%. A higher cardiothoracic ratio on chest x ray (HR 1.61; 95% CI 1.26 to 2.05, with 1 SD (6.2%) increase), a lower left ventricular ejection fraction (HR 1.42; 95% CI 1.20 to 1.69, with 1 SD (13%) decrease) and the presence of left bundle branch block (HR 3.14; 95% CI 1.28 to 7.71) were independently associated with a poorer prognosis, whereas the presence of apical hypertrophy at baseline (HR 0.58; 95%CI 0.36 to 0.92) predicted a better chance of survival.
Conclusions: The nationwide survey of patients with hypertrophic cardiomyopathy yielded important information on its prognosis and prognostic factors. These observations afford, for the first time, a measure of risk stratification in patients with HCM in Japan.

Hypertrophic cardiomyopathy (HCM) is a relatively common cardiac disease that has been the subject of intense investigation over the past few decades, especially in Western populations.[1–5] By contrast, few large-scale and prospective studies have been conducted to examine the prognosis and prognostic factors of HCM in the far-east Asian populations. Asian patients may differ considerably from Western patients in the pattern of hypertrophy distribution and clinical manifestations.[1 6] Because of marked heterogeneity in clinical expression, it is necessary to identify the prognostic factors and their association with death, within the broad disease spectrum of HCM, to obtain a realistic clinical perspective in the far-east Asians.

In 1999, the Japanese research committees on epidemiology of intractable diseases undertook a nationwide epidemiological survey of idiopathic cardiomyopathy in Japan to describe the detailed clinicoepidemiological features for appropriate health service planning. A detailed description of the clinicoepidemiological features of patient characteristics have been presented elsewhere.[7] The estimated total number of patients with HCM was 21 900 (95% confidence interval (CI) 20 600 to 23 200), with a crude prevalence rate of 17.3/100 000.[8] The purpose of this study was to evaluate the 5-year survival rate according to the presence and/or level of baseline prognostic factors from this nationwide study on patients with HCM in Japan, and to clarify factors that can predict the prognosis of this disease independently and effectively.

METHODS

The nationwide survey on cardiomyopathies, including HCM, was designed to show the prevalence and clinical features of HCM in Japan. Detailed methods have been described elsewhere.[7 8] The Japanese Research Committee on idiopathic cardiomyopathies prepared classification criteria, which were on the basis of the report of the World Health Organization/International Society and Federation of Cardiology task force on the definition and classification of cardiomyopathies.[9 10] HCM was characterised by disproportionate hypertrophy of the left ventricle and occasionally also of the right ventricle, which typically involves the septum more than the free wall, but occasionally is concentric. Specific heart muscle disease, defined as heart muscle disease of known aetiology or associated with disorders of other systems, was excluded from the survey. The hospitals included in each survey were randomly selected by stratified sampling of all departments of internal medicine, cardiovascular medicine and paediatrics throughout Japan, identified in a directory of names, department addresses and number of hospital beds obtained from the Ministry of Health and Welfare in Japan.

Data acquisition

The survey investigated patients with HCM as either inpatients or outpatients in the randomly selected departments in 1998. Firstly, the questionnaire for the survey on the number of patients with HCM was mailed directly to 2414 departments in January 1999. Of those 2414 departments, 1409 (58.4%) departments responded, reporting data on 7262 patients. The second survey was performed to collect detailed clinical data. From a total of 577 departments that reported one or more patients with HCM in the first survey, 235 departments agreed to participate in the second survey and detailed clinical data were collected from a total of 2155 patients. Patients who died before 1998 or those visiting a hospital for the first time after

Abbreviations: AF, atrial fibrillation; BMI, body mass index; HCM, hypertrophic cardiomyopathy; IVS, interventricular septum; LBBB, left bundle branch block; LVEF, left ventricular ejection fraction; LV, left ventricular; NYHA, New York Heart Association

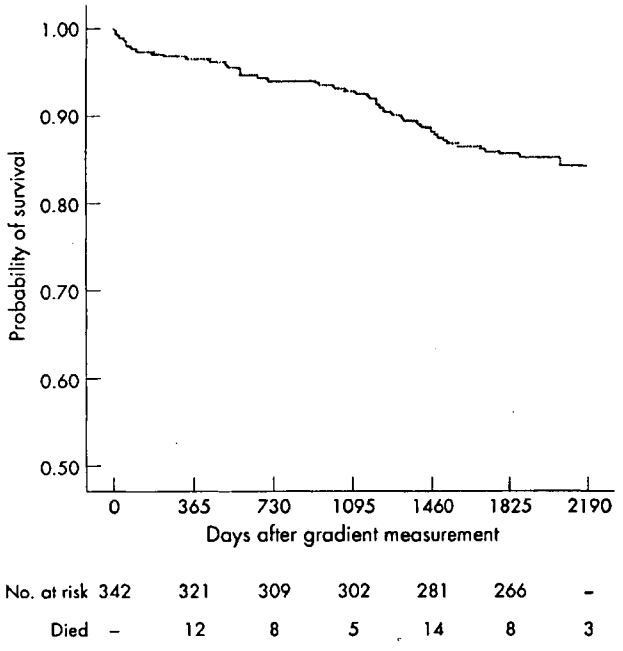

Figure 1 Kaplan–Meier survival curve of 342 patients with hypertrophic cardiomyopathy after first diagnosis in 1998.

1999 were excluded from this study as inappropriate cases, as were patients whose data were reported from more than one department (duplicate cases). The questionnaire requested detailed clinicoepidemiological information for each patient, including age, sex, symptoms and New York Heart Association (NYHA) functional class. Data from a physical examination and baseline laboratory measurements, including standard 12-lead ECG, chest *x* ray and echocardiography (for measuring left ventricular ejection fraction (LVEF), thickness of interventricular septum (IVS), and left ventricular (LV) shape), were available. LV hypertrophy by ECG was determined by left high voltage (Minnesota code: 3–1 or 3–3). M mode echocardiographic assessment for LVEF and two dimensional echocardiographic assessment for maximum IVS thickness and LV shape were conducted for nearly all patients. Apical hypertrophy was defined as LV wall thickness confined to the most distal region at the apex below the papillary muscle level. Data on blood tests and cardiac catheterisation were only obtained for a small portion of the subjects and, therefore, we did not include them in our analysis.

Medication

Patients were generally given medical treatment as reported previously from this study.[7] Medical treatment was directed toward control of symptoms, arrhythmias, coexisting hypertension and prevention of embolisation.

Follow-up

Of 235 departments reporting 2155 patients, 182 departments (reporting 1693 patients) agreed to participate in the 5-year follow-up survey. Patients' vital status was reported by doctors, with vital status for 607 withdrawn cases obtained from the residence-based register of the local government for each patient. However, follow-up was not possible for 88 patients, so these patients were excluded. Therefore, the 5-year follow-up was completed for 1605 (74.5%) patients. With regard to follow-up bias, we found no significant difference for sex, age, body mass index (BMI) and NYHA functional class distribution between those who participated and those who did not participate in the follow-up. The ethical committees of the Kanazawa Medical University and the Kyoto University Graduate School of Medicine approved the study protocol.

Statistical analysis

Survival estimates were calculated using the Kaplan–Meier method, and the 5-year survival probability was calculated for the overall cohort. Patients were classified on the basis of baseline prognostic factors. The significant differences in survival rates among classifications were tested by the log rank test for trends. Hazard ratios (HRs) according to baseline characteristics were calculated by Cox's proportional hazard model, with 95% CI up to the longest follow-up time of 2190 days. The model includes variables with a p value <0.05 by the log rank test for the 5-year survival and some other important variables. HRs for continuous variables were reported for 1 SD change. The log minus log plotted against survival time for each covariate did not show any deviation from the proportionality assumption. The data were analysed with SPSS V.12.0J. All reported significance levels are $p<0.05$ (two tailed tests).

RESULTS

Of the 1605 patients identified at baseline, 241 (15%) died during the follow-up period. The probability of actuarial survival was calculated from the time of the baseline survey for 342 patients who were initially diagnosed in 1998 (fig 1). The crude 5-year survival rate for those diagnosed in 1998 was 86% (95% CI 82 to 90). The crude 5-year survival rate for the whole cohort was 86% (95% CI 84 to 88).

Table 1 shows the baseline characteristics of the patients. Of the 1605 patients in the study, 30.3% were women and 57.1% were aged >60 years. Most patients (94.5%) had experienced none or only mild symptoms (NYHA function classes I or II) at baseline.

Clinical, echocardiographic and standard 12-lead ECG variables were examined for an association with survival during the follow-up period (table 1). Crude 5-year survival rates significantly decreased with decreasing BMI, higher grade of NYHA classification, presence of atrial fibrillation (AF) or flutter, presence of left bundle branch block (LBBB), increasing CTR, decreasing LVEF and decreasing number of hospital beds. The presence of apical hypertrophy was associated with a better survival rate. There was no significant difference in the crude survival rate between men and women. Thickness of IVS, family history of HCM, the presence or absence of hypertension, and smoking and drinking habits were not associated with the 5-year survival rates.

Table 2 presents the results of proportional hazard analysis. The model includes nine variables, which were statistically significant in table 1 (age, BMI, diabetes mellitus, NYHA classification, rhythm, LBBB, apical hypertrophy, CTR and LVEF), and two other important variables (sex and IVS thickness). The multivariate-adjusted HR for all-cause mortality was not significantly different between men and women. The presence of LBBB was an independent predictor of death (HR = 3.14), and the presence of apical hypertrophy, seen in 41.1% of study patients, resulted in a better prognosis (HR = 0.58). The multivariate-adjusted HR for death significantly and independently increased with a 1 (6.2%) SD increase of CTR, and with a 1 (13%) SD decrease of LVEF. The Wald statistic showed that these two factors had the strongest relationship with prognosis of all the factors in the model. BMI and IVS thickness were not independently related to prognosis. A backward elimination stepwise analysis to check if there is confounding among the non-significant factors, did not find a significant difference with the results in the original model.